JACS
JOURNAL OF THE AMERICAN CHEMICAL SOCIETY

pubs.acs.org/JACS
Article

Dynamin-like Proteins Combine Mechano-constriction and Membrane Remodeling to Enable Two-Step Mitochondrial Fission via a "Snap-through" Instability

Haleh Alimohamadi, Elizabeth Wei-Chia Luo, Xiaoying Liu, Wasi Iqbal, Rena Yang, Shivam Gupta, Kelsey A Nolden, Taraknath Mandal, R. Blake Hill, Liting Duan, and Gerard C. L. Wong*

Cite This: https://doi.org/10.1021/jacs.5c06352
Read Online

ABSTRACT: Mitochondrial fission is controlled by dynamin-like proteins, the dysregulation of which is correlated with diverse diseases. Fission dynamin-like proteins are GTP hydrolysis-driven mechanoenzymes that self-oligomerize into helical structures that constrict membranes to achieve fission while also remodeling membranes by inducing negative Gaussian curvature, which is essential for the completion of fission. Despite advances in optical and electron imaging technologies, the underlying mechanics of mitochondrial fission remain unclear due to the multiple times involved in the dynamics of mechanoenzyme activity, oligomer disassembly, and membrane remodeling. Here, we examine how multiscale phenomena in dynamin Drp1 synergistically influence membrane fission using a mechanical model calibrated with small-angle X-ray scattering structural data and informed by a machine learning analysis of the Drp1 sequence, and tested the concept using optogenetic mechanostimulation of mitochondria in live cells. We find that free dynamin-like proteins can trigger a "snap-through instability" that enforces a shape transition from an oligomer-confined cylindrical membrane to a drastically narrower catenoid-shaped neck within the spontaneous hemi-fission regime, in a manner that depends critically on the length of the confined tube. These results indicate how the combination of assembly and paradoxically disassembly of dynamin-like proteins can lead to diverse pathways to scission.

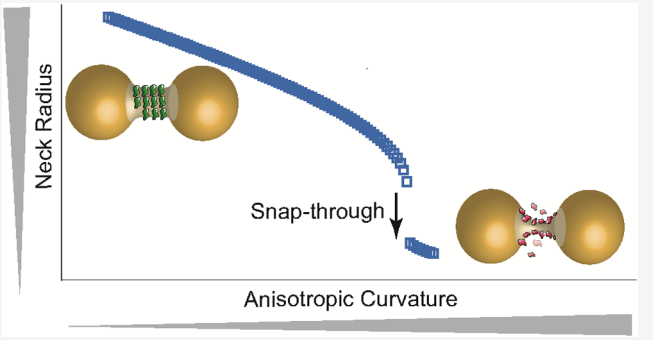

INTRODUCTION

The balance between the two antagonistic processes of mitochondrial fission and fusion is crucial in regulating the morphology and intracellular size distribution of mitochondria.[1−3] Defects or disruptions of this balance impact metabolism and apoptosis and have been correlated to developmental defects, cancer, cardiovascular diseases, and neurodegenerative diseases such as Parkinson, Alzheimers, Huntington, and amyotrophic lateral sclerosis (ALS).[4−6] The process of mitochondrial fission, in which a single mitochondrion divides into two separate daughter mitochondria, is facilitated by dynamin-related GTPase (Dnm1) in yeast and its conserved human homologue (Drp1).[1,7−10] Dnm1/Drp1 are GTPases from the dynamin-superfamily compromising of an N-terminal GTPase domain, a stalk or assembly domain, and an intrinsically disordered variable domain (IDVD).[2,11] In the current model, Dnm1/Drp1 is generally acknowledged to oligomerize at the mitochondrial membrane surface, forming helical structures with an outer diameter of ∼50 nm, with the GTPase domains facing the outside, and the IDVD domains on the inside, in contact with the mitochondrial membrane.[12−14] Upon nucleotide hydrolysis, the Dnm1/Drp1 helical structures undergo a conformational change, locally constricting the mitochondrial membranes into a nanoscopic tube, and acts as a GTP hydrolysis-driven effector of fission.[12,15,16] Interestingly, it has been experimentally observed that GTP hydrolysis also promotes disassembly of the oligomeric, confining helix.[17−19] At present, the precise mechanism of mitochondrial fission is still a matter of debate considering constriction does not appear to lead deterministically to scission.[12]

There are two main classes of extant models for Dnm1/Drp1 driven fission.[12] In "two-step models", nucleotide-loaded assembles of dynamin-like proteins into helical structures, forming a scaffold around the mitochondrion to create a confined lipid tubule.[12,14,20] GTP hydrolysis induces the

Received: April 15, 2025
Revised: June 3, 2025
Accepted: June 11, 2025

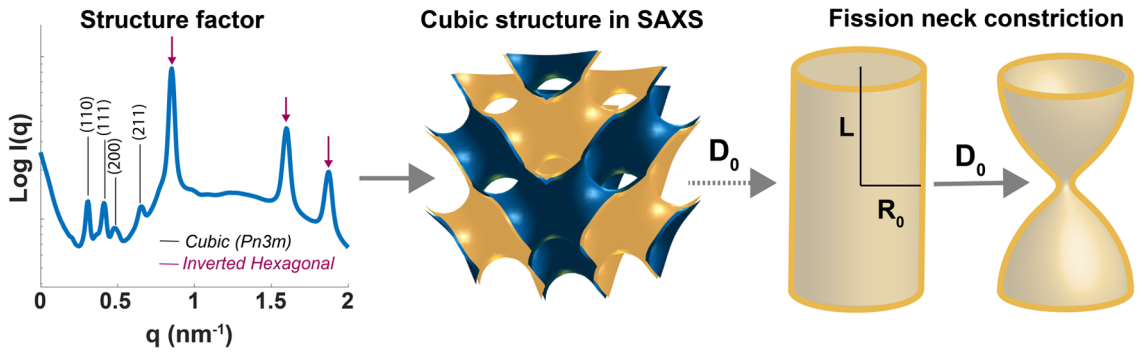

Figure 1. Using induced membrane curvature deformations by dynamin-related proteins in SAXS spectra to estimate the radius of mitochondrial fission. Correlation peaks corresponding to reflection peaks are indicated for cubic (black lines) and inverted hexagonal (red) phases. The magnitude of generated anisotropic curvature by dynamin-like proteins in cubic phases is used as an input for the mechanical model, constricting a tubular membrane with a radius of R_0 = 20 nm and a half-length of L.

subsequent disassembly of Dnm1/Drp1 oligomers[17−19] leading to the formation of hemi-fission intermediates and eventual scission.[12,14,20] This composite process occurs via two time scales, a slow one for the confinement and a fast one for the final scission. In contrast, for "constrictase models", Dnm1/Drp1 acts like a molecular motor that enforces stepwise sliding of adjacent helical turns, leading to actively increasing degrees of constriction that itself leads to scission.[12] Both models have their own explanatory power and limitations.[12]

Before we consider how to parse the various features of these models, it is important to examine how drastically different physical mechanisms exert their contrasting influences on a mitochondrial membrane. For example, using coarse-grained molecular dynamic simulations, Pannuzzo et al. have proposed that the rotation of mitochondrial dynamin-like proteins filaments around their longitudinal axis induces a local torque, which can trigger the topological transition of mitochondria into the hemi-fission state.[22] In the continuum framework, previous studies have suggested that the localization of conical lipids in the pinching domain and the nonaxisymmetric collar pressure induced by the helical arrangement of dynamin-like proteins facilitate the membrane scission process and stabilize the highly constricted necks.[21,23] Utilizing theoretical models and experimental measurements of ionic conductivity in a tubular membrane connected two parallel axisymmetric rings, Frolov et al. have demonstrated there is a critical tubule length at which the tubule transitions from a cylindrical nanotubule to a catenoid in less than a millisecond.[24] To compound these already complex phenomena, it has been noted that dynamin-like proteins can induce negative Gaussian curvature (NGC) in membranes, the type of curvature necessary for scission.[25]

Here we provide a conceptual framework that combines a theoretical mechanical model with small-angle X-ray scattering (SAXS) structural data (Figure 1) to reconcile the two types of models and show how constrictase activity and hydrolysis driven disassembly synergistically contribute to fission. Our approach reveals the critical roles played by dynamin dynamic assembly and disassembly of dynamin-like proteins and reconciles the two extant classes of models for the first time in a new framework. Specifically, we find that free dynamin-like proteins can induce an unanticipated "snap-through instability" that triggers a rapid shape transition from a cylindrical membrane tube to a highly constricted catenoid-shaped neck. This transition occurs within the range of the spontaneous hemi-fission regime. Importantly, whereas many studies have focused on the role played by the width of the dynamin-like protein oligomer confined membrane tube, we find that the length of the confined membrane tube is critically important: the occurrence of the snap-through transition induced by free dynamin-like proteins depends strongly on this length. We also show that the large anisotropic bending rigidity in conjunction with a high membrane tension facilitates the mitochondrial fission process. These results suggest that the mechanoenzyme activity of dynamin-like proteins—forming sufficiently long nanoscopic tubes through oligomeric constrictase action—can synergize with the generation of negative Gaussian curvature (NGC) following oligomer disassembly and the release of monomers. This synergy provides a foundation for reconciling existing models of mitochondrial fission. Finally, we apply our framework to compare the radius of fission necks induced by Dnm1 and Drp1 in various lipid compositions. Our results show that both Dnm1 and Drp1 can consistently induce narrow and robust necks in the hemi-fusion range, for lipid membranes with a high percentage of cardiolipin. This behavioral trend with cardiolipin from our data-calibrated mechanical model is consistent with previous experimental studies.[26−28] Using coarse-grained molecular dynamics simulations, we also illustrate that the Dnm1/Drp1 complex can induce large anisotropic curvature in membranes with higher cardiolipin content. We think that our mechanical framework can be generalized to a broader range of protein-based fission machinery that can generate NGC on the membrane.

RESULTS AND DISCUSSION

Membrane Mechanics. Our system comprises a tubular lipid membrane and rigid curvature-inducing dynamin-related GTPase proteins that are embedded in the membrane surface. We model the lipid bilayer as an elastic shell with negligible thickness compared to its bending.[29,30] This allows us to describe the geometry of the membrane in terms of its mean (H) and deviatoric (D) curvatures, defined as[31,32]

$$H = \frac{c_1 + c_2}{2} \qquad D = \frac{c_1 - c_2}{2} \tag{1}$$

where c_1 and c_2 are the principal curvatures of the surface (Figure 2A). Distinct combinations of these curvatures give rise to characteristic surfaces, such as spherical buds and catenoid-shaped necks. For example, for an isotropic-shaped spherical bud with $c_1 = c_2 = 1/R_{bud}$ (Figure 2A), $H = \frac{1}{R_{bud}}$ and

https://doi.org/10.1021/jacs.5c06352
J. Am. Chem. Soc. XXXX, XXX, XXX−XXX

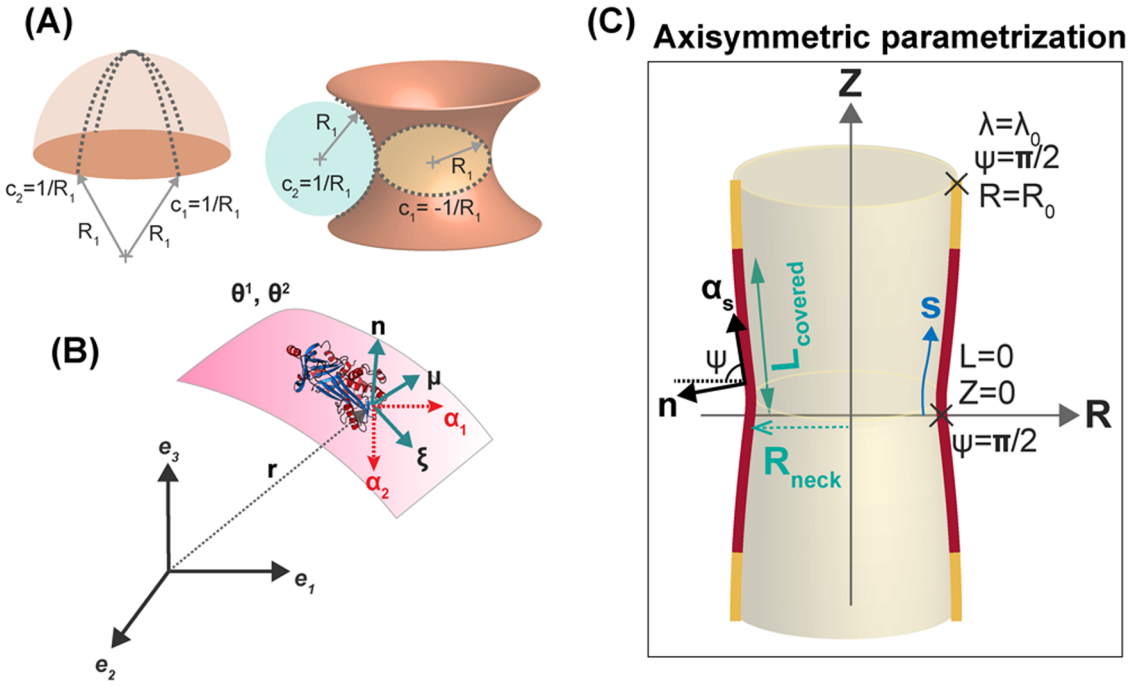

Figure 2. (A) Schematic illustrating the principal curvatures on spherical and catenoid-shaped surfaces. (B) Coordinate system used to define the membrane surface. Tangent basis $\boldsymbol{a}_1$, $\boldsymbol{a}_2$ are constructed at any point using the position vector $\boldsymbol{r}$, as $\boldsymbol{a}_\alpha = \boldsymbol{r}_{,\alpha}$ where $\alpha \in \{1, 2\}$ and $(.)_\alpha$ is the partial derivative. The normal vector is defined $\boldsymbol{n} = \boldsymbol{a}_1 \times \boldsymbol{a}_2/|\boldsymbol{a}_1 \times \boldsymbol{a}_2|$, and $\boldsymbol{\xi}$ is the unit vector representing orientation of protein in the tangential plane. $\boldsymbol{\mu}$ is defined as $\boldsymbol{\mu} = \boldsymbol{n} \times \boldsymbol{\xi}$. (C) The surface parametrization of the tubular membrane with a radius of R_{neck} in axisymmetric coordinates and the prescribed boundary conditions. The yellow region represents the bare membrane, and the red region with a length of $L_{covered}$ is the domain covered by dynamin s is the arc length, $\boldsymbol{n}$ is the unit normal vector to the surface, $\boldsymbol{a}_s$ is the unit tangent vector in the direction of arc length, and ψ is the angle made by the tangent vector with respect to its radial plane.

$D = 0$. However, in the case of an anisotropic catenoid-shaped neck with $c_1 = -c_2 = 1/R_{neck}$ (Figure 2A), $H = 0$ and $D = \frac{1}{R_{neck}}$.

We used the modified version of Helfrich energy that includes the deviatoric components to model the bending energy density of the membrane (W), given as[33−38]

$$W(H, K, \theta^\alpha) = \kappa(H - C_0)^2 + \kappa_2(D - D_0)^2 \tag{2}$$

where κ is the membrane bending rigidity associated with isotropic curvature and κ_2 is the membrane bending rigidity associated with anisotropic curvature. θ^α represents the surface coordinate where $\alpha \in \{1, 2\}$ (Figure 2B). C_0 is the induced spontaneous isotropic and D_0 is the induced deviatoric curvatures by dynamin-related GTPase proteins. Assuming $c_{1,p}$ and $c_{2,p}$ are the curvatures induced by dynamin-like proteins in the two principal directions, $C_0 = \frac{c_{1,p} + c_{2,p}}{2}$ and $D_0 = \frac{c_{1,p} - c_{2,p}}{2}$.[39,40] As an illustration, C_0 captures the curvatures induced by proteins that form spherical coats, such as clathrin, while D_0 represents the curvatures induced by proteins such as BAR domains and dynamin-like proteins, which form tubular and neck-shaped structures.[41] It should be mentioned that, with no induced curvatures ($C_0 = 0$ and $D_0 = 0$), eq 2 reduces to the classical Helfrich energy with quadratic dependence on mean curvature and linear dependence on Gaussian curvature, where κ_2 represents the magnitude of the Gaussian modulus, $\kappa_2 = -\kappa_G$ (more details in the supplement).

Assuming the membrane is inextensible and the whole system of membrane and proteins is in mechanical equilibrium at all times, the normal force balance leads to the "shape equation" given as[34,42,43]

$$\underbrace{\frac{1}{2}[W_D(\xi^\alpha\xi^\beta - \mu^\alpha\mu^\beta)]_{\beta\alpha} + \frac{1}{2}W_D(\xi^\alpha\xi^\beta - \mu^\alpha\mu^\beta)b_{\alpha\gamma}b^\gamma_\beta + \Delta\left(\frac{1}{2}W_H\right) + W_H(2H^2 - K) - 2HW}_{\text{Elastic effects}} = \underbrace{p + 2H\lambda}_{\text{Capillary effects}} + \underbrace{\boldsymbol{\tau}.\boldsymbol{n}}_{\text{Compressive stress induced by dynamin}} \tag{3}$$

where ξ^α and μ^α are the projections of $\boldsymbol{\xi}$ and $\boldsymbol{\mu}$ along the tangent vector on the surface. Here, $\boldsymbol{\xi}$ is a unit vector representing the orientation of protein, and $\boldsymbol{\mu}$ is defined as $\boldsymbol{\mu} = \boldsymbol{n} \times \boldsymbol{\xi}$ where $\boldsymbol{n}$ is the unit surface normal[37] (Figure 2B). $b_{\alpha\gamma}$ is the coefficients of the second fundamental form, b^γ_β is the mixed components of the curvature, and $(.)_{;\alpha}$ is the covariant derivative. W_D and W_H are the partial derivatives of energy density W, and K is the Gaussian curvature ($D^2 = H^2 - K$). Δ is the surface Laplacian, λ is the Lagrange multiplier for the area constraint interpreted to be the membrane tension, and p is the pressure difference across the membrane. $\boldsymbol{\tau}$ is the compressive force density on the membrane induced by helical arrangements of dynamin-like proteins.[34] In the absence of elastic effects and compressive stress, the membrane shape eq (eq 3) simplifies to the well-known Young−Laplace equation for soap bubbles, where the osmotic pressure is balanced by surface tension.

https://doi.org/10.1021/jacs.5c06352
J. Am. Chem. Soc. XXXX, XXX, XXX−XXX

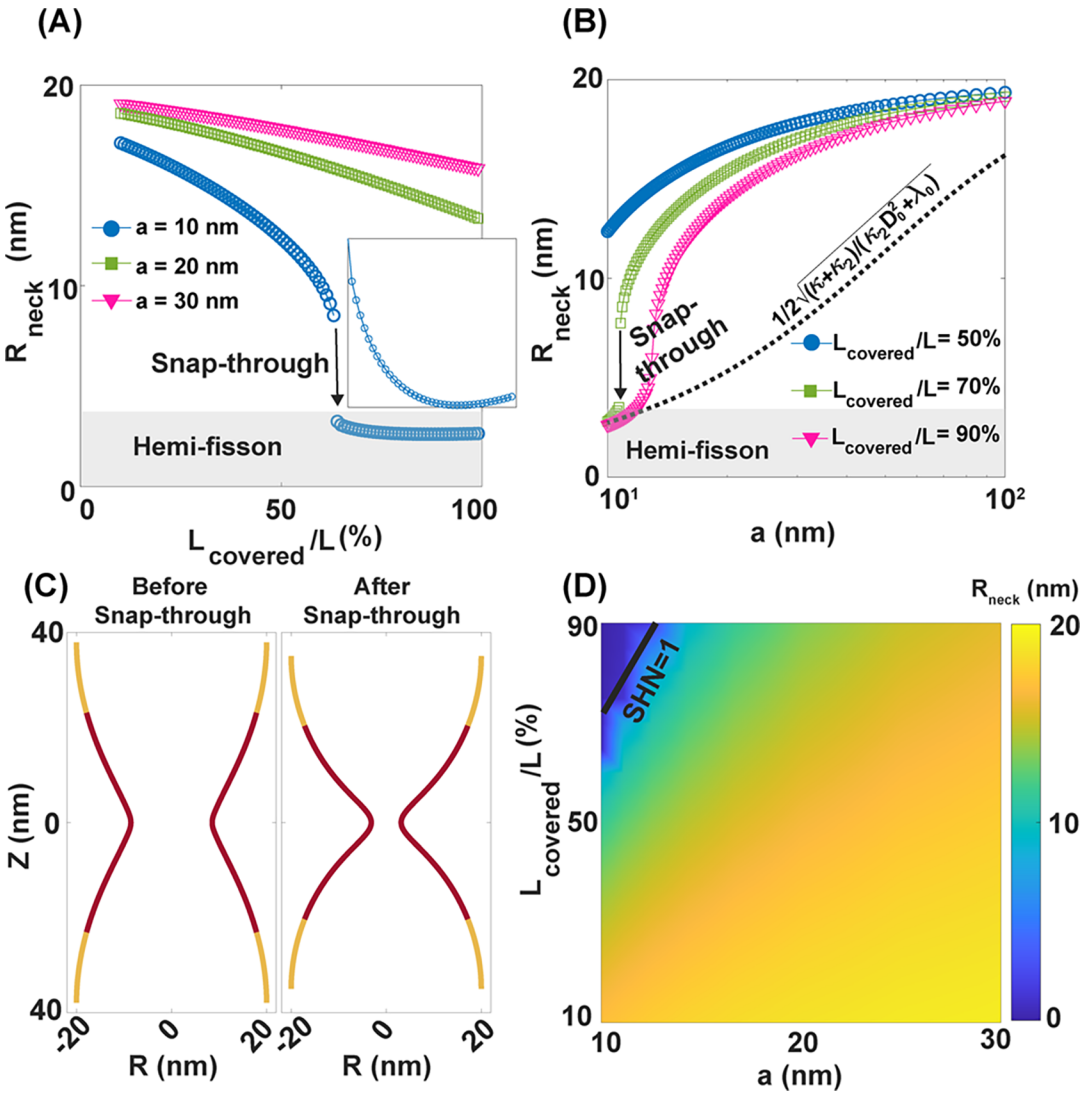

Figure 3. Estimating the radius of the mitochondrial fission neck by dynamin-related proteins using the lattice constant of induced cubic structures in SAXS experiments. (A) The radius of the mitochondrial constricted neck as a function of protein coverage for three different cubic lattice constants. For a small lattice constant, there is a snap-through transition from a wide to narrow neck with increasing protein coverage. (B) Radius of the mitochondrial constricted neck as a function of the cubic lattice constant for three different protein coverages. As the lattice constant of the cubic phase decreases, the neck becomes narrower. The dotted black line represents to the analytical solution for the equilibrium radius of a tubular membrane in the presence of deviatoric curvature, given as $R_{tube} = 1/2\sqrt{(\kappa + \kappa_2)/(\kappa_2 {D_0}^2 + \lambda_0)}$.[34] (C) The morphology of the constricted neck before and after the snap-through transition with a fixed a = 10 nm. (D) Phase diagram of the constricted neck for a range of cubic lattice constants and protein coverages. The solid black line indicates SHN = 1, above which R_{neck} < 3 nm within the spontaneous hemi-fission regime. $k_2/k = 1$, $\lambda_0 / \lambda_{cylinder} = 1$, and $L/R_0 = 2$.

A balance of forces tangent to the membrane yields the spatial variation of membrane tension given as[34,42−44]

$$\lambda_{,\alpha} = -W_{,\alpha|\mathrm{exp}} - \boldsymbol{\tau}.\,\mathbf{a}_{\alpha} \tag{4}$$

where $(.)_{\alpha}$ is the partial derivative, $(.)_{|\mathrm{exp}}$ denotes the explicit derivative with respect to coordinate, and $\boldsymbol{a}_{\alpha}$ is a tangent vector on the surface (Figure 2B). For a homogeneous membrane with no protein distribution on the surface, eq 4 simplifies to λ = constant everywhere, representing the membrane tension required to maintain a tubular shape. The Supporting Information provides a detailed derivation of the force balance's governing equations and the procedure for non-dimensionalization.

The magnitude of induced deviatoric curvature (D_0) in eq 2 can be estimated from the cubic structure formed by dynamin-related proteins in SAXS, given as[45,46]

$$D_0 = \langle D_{\mathrm{cubic}} \rangle = \sqrt{\frac{2\pi\chi}{A^* a^2}} \tag{5}$$

where $\langle D_{\mathrm{cubic}} \rangle$ is the average membrane curvature deviator in a cubic phase, a is the lattice constant of the cubic phase, χ is the Euler characteristic, and A^* is the surface area per unit cell specific to each cubic phase.[47,48]

Numerical Implementation. For simplicity in the numerical calculations, we modeled the confined mitochondrial membrane as a tubular lipid bilayer that is rotationally symmetric and also has a reflection symmetry with respect to the Z = 0 plane (Figure 2C). This allows us to define the

https://doi.org/10.1021/jacs.5c06352
J. Am. Chem. Soc. XXXX, XXX, XXX−XXX

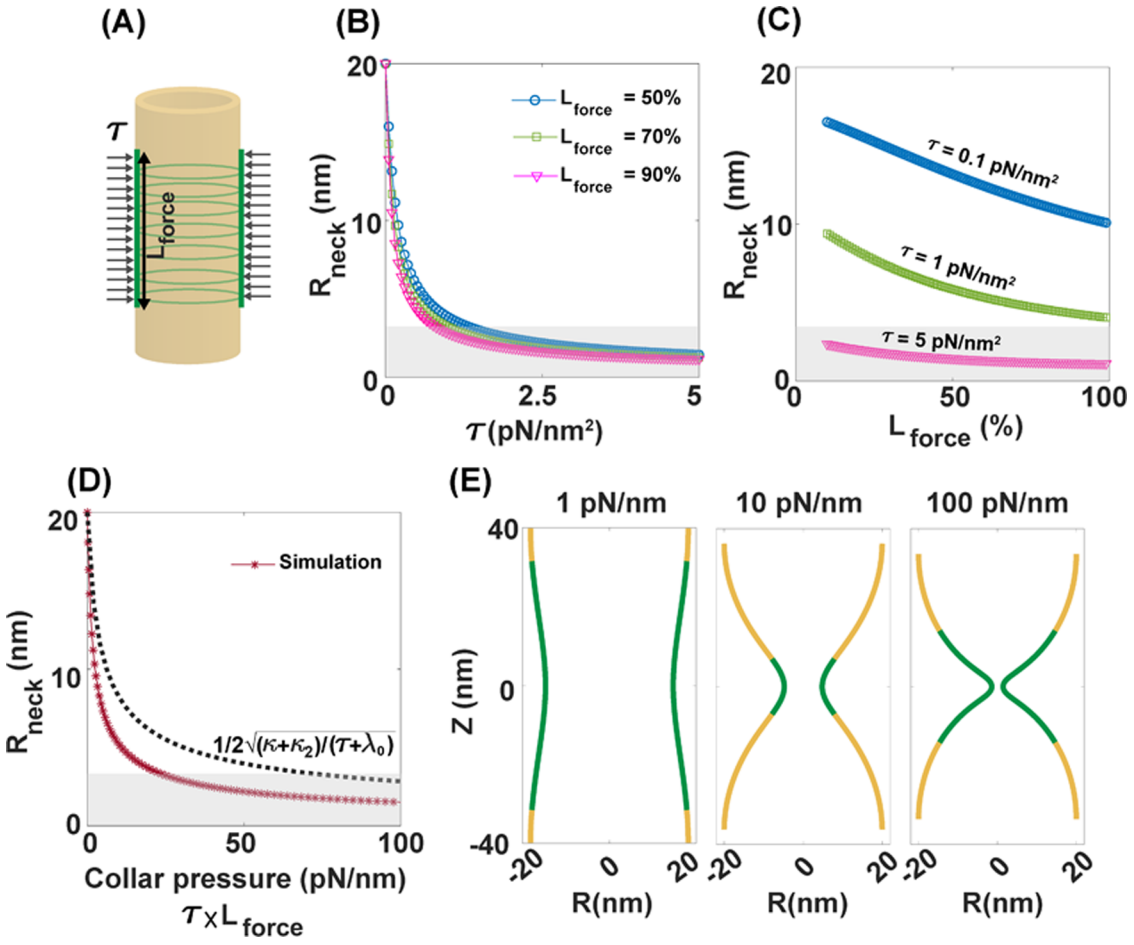

Figure 4. Continuous constriction of the mitochondrial fission neck by compressive forces induced by dynamin helical rings ($D_0 = 0$). (A) Radius of the mitochondrial constricted neck as a function of the compressive force density for three different lengths of the applied force. The inset shows the schematic of a tubular membrane with a uniform compressive force density ($\boldsymbol{\tau}$) applied over a length of L_{force} shown in green. (B) The radius of the mitochondrial constricted neck as a function of the collar pressure defined as $\tau \times L_{force}$. The radius of the neck falls below the threshold for spontaneous hemi-fission for collar pressure >75 pN/nm. The dotted black line corresponds to the analytical solution for the equilibrium radius of a tubular membrane under a uniform force density, given as $R_{tube} = 1/2\sqrt{(\kappa + \kappa_2)/(\tau + \lambda_0)}$. (C) The morphology of the constricted neck with three different magnitudes of applied collar pressure. $k_2/k = 1$, $\lambda_0/\lambda_{cylinder} = 1$, and $L/R_0 = 2$.

surface of revolution as $\boldsymbol{r}(s) = R(s)\boldsymbol{e}_r + Z(s)\boldsymbol{k}$, where s is the arc length along the curve, where $\boldsymbol{e}_r$ and $\boldsymbol{k}$ are the coordinate basis, $R(s)$ is the radial distance from axis of revolution and $Z(s)$ is the elevation from the reference plane (Figure 2C).[49,50] We also define the normal and tangential vectors to the surface as $\boldsymbol{n} = -\sin(\psi)\boldsymbol{e}_r + \cos(\psi)\boldsymbol{k}$ and $\boldsymbol{a}_s = \cos(\psi)\boldsymbol{e}_r + \sin(\psi)\boldsymbol{k}$, where ψ is defined as the angle between the tangent and the horizontal axis (Figure 2C). This parametrization reduces the membrane shape equation (eq 3) and the tangential force balance equation (eq 4) to a coupled system of first-order differential equations (eq S13). Having the amount of induced deviatoric curvature from SAXS data (eq 5) as an input, we used "bvp4c", a boundary value problem solver in MATLAB, to solve this system of equations coupled with the prescribed boundary conditions shown in Figure 2C (eqs S17 and S18).[51] In our simulations, we set $\kappa = 30kT$[52] to mimic the bending rigidity of mitochondrial membrane and started from a tubular membrane with a radius of $R_0 = 20$ nm[18,53,54] and a half-length of L (Figure 2C). We also set $p = 0$ to focus only on the mechanism of dynamin-related proteins in governing the mitochondrial fission process. Additionally, we set $C_0 = 0$ to model the formation of catenoid-shaped necks by dynamin-related proteins, which exhibit minimal spontaneous curvature and maximal local negative Gaussian curvature (NGC), driving the final step of mitochondrial fission.

Induced Anisotropic Curvature by Molecular Motor Dynamin-like Proteins Can Drive Spontaneous Mitochondrial Fission via a Snap-through Transition. The dynamin family of proteins can constrict tubular membranes to form narrow necks. The size of these necks is a key geometric parameter that controls the dynamics of mitochondrial division, including the spontaneous fission process and the fission time from a few seconds to a couple of minutes.[12,55] Here, we use our mechanical framework to understand how (i) the lattice constant of the induced cubic phases by dynamin-like proteins, as observed in SAXS measurements,[25] and (ii) the area of membrane tubule covered by dynamin-like proteins ($L_{covered}$) are correlated to the size of the mitochondrial constricted necks (Figure 2C). To do that, we started from a tubular membrane with $R_0 = 20$ nm, $L/R_0 = 2$ and set $\kappa_2/\kappa = 1$. In mechanical equilibrium and with no deviatoric curvature, the membrane tension required to maintain a tubular membrane ($\lambda_{cylinder}$) depends on the bending rigidities and

https://doi.org/10.1021/jacs.5c06352
J. Am. Chem. Soc. XXXX, XXX, XXX−XXX

the tubule radius as $\lambda_{cylinder} = (\kappa + \kappa_2)/4R_0^2$ (eq S20)[34,56] and set the tension at the boundary is set $\lambda_0 = \lambda_{cylinder}$.

In Figure 3A, we plot the radius of the neck as a function of the protein coverage for three different $Pn3m$ cubic lattice constants, corresponding to different magnitudes of induced deviatoric curvature. We observed that, for large lattice constants, e.g., a = 20 and a = 30 nm, the radius of the neck continuously decreases with an increase in the percentage of protein coverage (Figure 3B). However, for a small lattice constant of a = 10 nm (large deviatoric curvature), the neck constriction with increasing protein coverage is associated with a snap-through transition from a wide neck ($R_{neck} \sim 8.5$ nm) to a narrow neck ($R_{neck} < 3$ nm) in the limit of spontaneous hemi-fission[57] (Figure 3A). The snap-through instability resembles the fast fission transition (less than 100 ms) induced by the GTP hydrolysis and disassembly of dynamin oligomers, as proposed in two-step dynamin-mediated fission model.[12] Interesting, we observed that after the snap-through transition there is a minimum neck size of $R_{neck} \sim 2.6$ nm, and then the size of the neck slightly increases with further increase in protein coverage (see the inset in Figure 3A).

We also plotted the radius of the mitochondrial neck as a function of the lattice constant of the $Pnm3$ cubic phase for three different percentages of protein coverage. We observed that the radius of the neck decreases with the decrease in the cubic lattice constant (larger induced deviatoric curvature in eq 4). This is in agreement with the analytical solution for the equilibrium radius of a tubular membrane in the presence of spontaneous deviatoric curvature, given by $R_{tube} = 1/2\sqrt{(\kappa + \kappa_2)/(\kappa_2 D_0^2 + \lambda_0)}$[34] (dotted black line in Figure 3B). Based on the length of the protein coverage, we identified three regimes of neck constriction: (i) For small protein coverage ($L_{covered}/L$ = 50%), the neck constriction is smooth, and a decrease in the cubic lattice constant from a = 100 nm to a = 10 nm results in a ∼36% reduction in the neck radius from $R_{neck} \sim 20$ nm to $R_{neck} \sim 12.4$ nm (Figure 3B). (ii) For intermediate protein coverage ($L_{covered}/L$ = 70%), the neck constriction is associated with a snap-through transition and the radius of the neck decreases significantly, by ∼87%, reaching the spontaneous hemi-fission regime ($R_{neck} < 3$ nm) at small cubic lattice constants (Figure 3B). (iii) For large protein coverage ($L_{covered}/L$ = 90%), the radius of the neck decreases smoothly from $R_{neck} \sim 20$ nm to $R_{neck} \sim 2.6$ nm as the cubic lattice constant decreases from a = 100 nm to a = 10 nm (Figure 3B). The morphology of constricted membrane tubes before and after the snap-through transition is shown in Figure 2C. Before snap-through, the membrane tubule is constricted to a wide neck, whereas a narrow, catenoid-shaped neck forms after the snap-through transition (Figure 3C).

In Figure 3D, we plot a phase diagram of the radius of the constricted neck for a range of cubic lattice constants and protein coverage. To estimate the range of spontaneous hemi-fission regime based on the magnitude of cubic lattice constant and the length of the protein coverage, we introduced a dimensionless quantity, the spontaneous hemi-fission number $SHN = \frac{\kappa_2 L \lambda_0}{4\kappa R_0 \lambda_{cylinder}} \left(\frac{L_{covered}}{a}\right)^2$. Based on our results, a SHN = 1 is a threshold for the formation of narrow necks, while a SHN > 1 corresponds to constricted necks within the spontaneous hemi-fission regime (above the solid black line in Figure 3D). Overall, these results suggest that the anisotropic curvature induced by dynamin-like proteins can remodel tubular membranes into narrow necks within the range of the spontaneous hemi-fission regime, and our model predicts that this transition can be discontinuous, occurring through a snap-through instability.

Collar Pressure Induced by Helical Arrangements of the Dynamin-like Proteins Smoothly Constricts Mitochondrial Membrane into Narrow Necks. It is well-known that the helical assembly of the dynamin family of proteins can squeeze mitochondrial membranes to narrow necks, thereby facilitating the fission process.[16,58−60] To compare the constriction mechanism of a tubular-shaped mitochondria by dynamin-induced anisotropic curvature (D_0) with the collar pressure generated by rings of the dynamin assembly (τ), we repeated the same simulation in Figure 3 with no deviatoric curvature (D_0 = 0). We assumed that the helical rings of dynamin generate a uniform compressive force density τ over a length of L_{force} on the tubular membrane (Figure 4A). We found that the compressive force density induced by the helical orientation of dynamin-like proteins can smoothly constrict the tubular membrane into a narrow neck, and the degree of the constriction slightly depends on the length of the applied force density (Figure 4A). This is consistent with the previous study by McDargh et al., that have suggested that the helical assembly of dynamin-like proteins does not destabilize membrane during mitochondrial fission.[61] Indeed, the smooth constriction is reminiscent of the slow pinching process (occurring over a period of seconds) that is mediated by dynamin scaffolding, as proposed in the two-step dynamin's fission model.[12] Based on our results, a compressive force density $\tau > 2.5$ pN/nm^2 is required to form narrow necks within the range of the spontaneous hemi-fission limit (Figure 4A).

We combined the effects of force density and the length of the applied force by defining collar pressure as $\tau \times L_{force}$. Based on our results, the radius of the neck decreases smoothly with an increase in the magnitude of the collar pressure, and a collar pressure >75 pN/nm is needed to form narrow necks ($R_{neck} <$ 3 nm) within the spontaneous hemi-fission regime (Figure 4B). The analytical solution for the equilibrium radius of a tubular membrane under uniform force density ($R_{tube} = 1/2\sqrt{(\kappa + \kappa_2)/(\tau + \lambda_0)}$, eq S22) is represented as a dotted black line (Figure 3B). For small collar pressures, there is good agreement between the analytical expression and numerical results (Figure 4B). However, for large collar pressures, when catenoid-shaped necks form, the analytical solution deviates from the simulation results (Figure 4B). In Figure 3C, we demonstrate the morphologies of the constricted tube by increasing the magnitude of the applied collar pressure. The green line indicates the domain of applied compressive force (Figure 4C). These results suggest that increasing either the local magnitude of compressive force (τ) or the length of dynamin polymerization (L_{force}) can lead to membrane scission. Overall, our findings in Figures 3 and 4 can provide insight into the driving mechanisms and the relative time scales in each step of the two-step model of dynamin-catalyzed fission.

Longer Mitochondrial Membranes Are Easier to Constrict by Dynamin-Induced Anisotropic Curvature. The length of tubular membranes formed by the dynamin helical structures can vary widely, ranging from nanometers to micrometers.[26,27] Additionally, dynamin oligomerization and membrane constriction elongate tubular membranes confined

https://doi.org/10.1021/jacs.5c06352
J. Am. Chem. Soc. XXXX, XXX, XXX−XXX

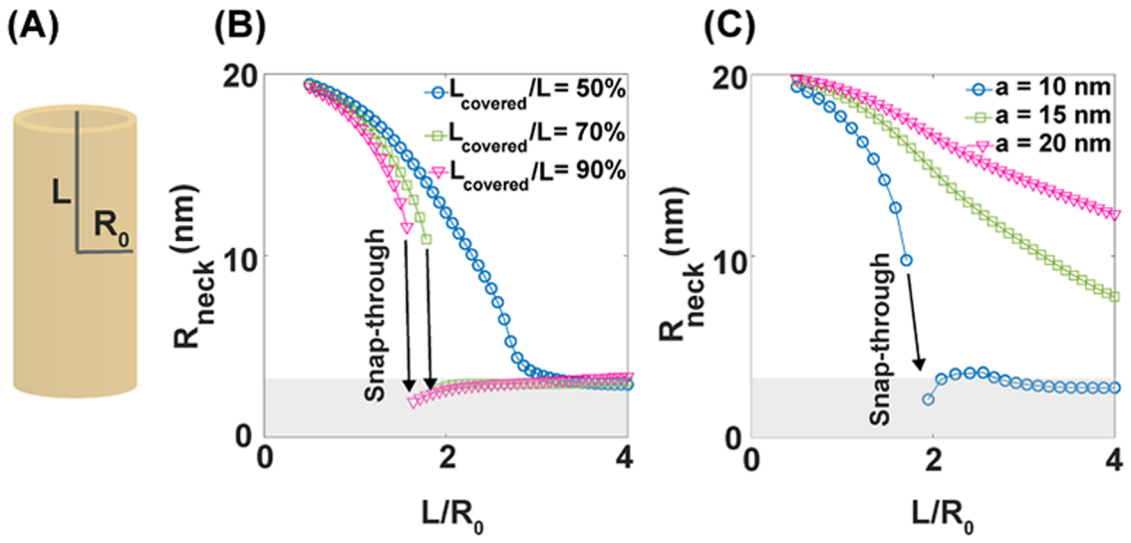

Figure 5. Length of mitochondria affects the efficiency of dynamin-induced curvature constriction. (A) Schematic representation of a tubular membrane with a radius of R_0 = 20 nm and a half-height of L. (B) The radius of the mitochondrial constricted neck as a function of the tubule height to the radius ratio (L/R_0) for three different protein coverages (a = 10 nm). For large protein coverage ($L_{covered}/L$ = 70% and 90%), there is a discontinuous transition from a wide neck to the hemi-fission regime with an increase in the height of the membrane tubule. (C) The radius of the mitochondrial constricted neck as a function of L/R_0 for three cubic lattice constants ($L_{covered}/L$ = 80%). For a small lattice constant (a = 10 nm), there is a discontinuous transition from a wide neck to the hemi-fission regime with an increase in the height of the membrane tubule. k_2/k = 1, and $\lambda_0/\lambda_{cylinder}$ = 1.

by dynamin scaffolding.[62] How does the length of the membrane tubule influence the mitochondrial fission rate? Using the mitochondrially targeted KikGR1 protein visualization technique, Cagalinec et al. have showed that in both cortical and cerebellar granule neurons, the mitochondrial fission rate increased dramatically in longer mitochondria, while the fusion rate was almost independent of length.[63] Berman et al. have also proposed a model to relate the probability of a fission event in a mitochondria to its length.[64] To explore the effect of mitochondria length on the constriction process induced by the dynamin family of proteins, we repeated the simulations in Figure 2 for a range of L/R_0 (fixed R_0 = 20 nm) from a short tubule (L/R_0 = 0.5) to a long one (L/R_0 = 4) (Figure 5). We found that the dynamin-induced anisotropic curvature (D_0) can constrict longer tubules more effectively than shorter ones (Figure 5B,C). For example, with a cubic lattice constant of a = 10 nm and $L_{covered}$ = 50%, the induced curvature slightly reduces the neck size of a short tubule with L/R_0 = 1 to $R_{neck} \sim$ 18 nm (Figure 5B). However, for a long membrane tube with L/R_0 = 4, the same curvature significantly constricts the tube into the spontaneous hemi-fission regime with R_{neck} < 3 nm (Figure 5B). This could be attributed to the greater bending moment (force × length) induced by curvature-generating proteins in longer membrane tubules, which resembles the easier bending of a longer beam in classical mechanics.

Interestingly, we observed that for large protein coverages and small cubic lattice constants, there is a snap-through transition in the radius of the constricted neck as L/R_0 increases (Figure 5B,C). Based on our results, the neck radius decreases smoothly when L/R_0 increases from L/R_0 = 0.5 to L/R_0 < 2. Then, it abruptly transitions into the spontaneous hemi-fission regime at $L/R_0 \sim$ 1.8, reaching the minimum neck size (Figure 5B,C). Beyond this point, the neck size slightly increases with larger L/R_0 ratios (Figure 4B,C). This snap-through instability resembles the spontaneous hemi-fission induced by GTP hydrolysis and sliding of adjacent turns of dynamin helices at a critical tubule length, as proposed in the constrictase dynamin's fission model.[12] Similarly, Frolov et al. have shown the shape bistability transition of cylindrical nanotubes into catenoidal microtubules is associated with an increase in the length of tubule lipid membranes.[24] To investigate the net effect of tubule height on the efficiency of curvature-induced constriction, we kept the length of protein coverage constant (e.g., $L_{covered}$ = 36 nm for all tubule heights which corresponds to 22.5% < $L_{covered}/L$ < 90%) and repeated the simulations (Figure S1). Consistently, we found that the same amount of anisotropic curvature leads to the formation of a narrower constricted neck in longer tubules compared to shorter ones (Figure S1). Thus, our mechanical framework suggests that longer mitochondrial membrane tubules formed by dynamin helicoidal assembly are susceptible to spontaneous hemi-fission triggered by dynamin-induced membrane remodeling machinery.

Interplay of Membrane Anisotropic Bending Rigidity and Tension Regulates the Dynamic of Mitochondrial Constriction by Dynamin-Induced Anisotropic Curvature. The bending rigidity of the membrane describes its resistance to bending, and it depends on the lipid composition of the membrane and the curvature generating proteins embedded within it.[65−67] It has been demonstrated both theoretically[68] and experimentally[67] that a more negative Gaussian modulus (larger k_2) in the protein-covered domain can facilitate membrane budding process and neck formation. However, measuring the Gaussian modulus of the lipid bilayer and protein composition at the neck domain remains challenging.[69] Here, to understand how the magnitude of the anisotropic bending modulus relative to the isotropic bending rigidity (k_2/k) affects the process of mitochondrial constriction by dynamin-induced deviatoric curvature, we conducted simulations across a wide range of k_2/k and with different protein coverages (Figure 6A, a = 10 nm).

https://doi.org/10.1021/jacs.5c06352
J. Am. Chem. Soc. XXXX, XXX, XXX−XXX

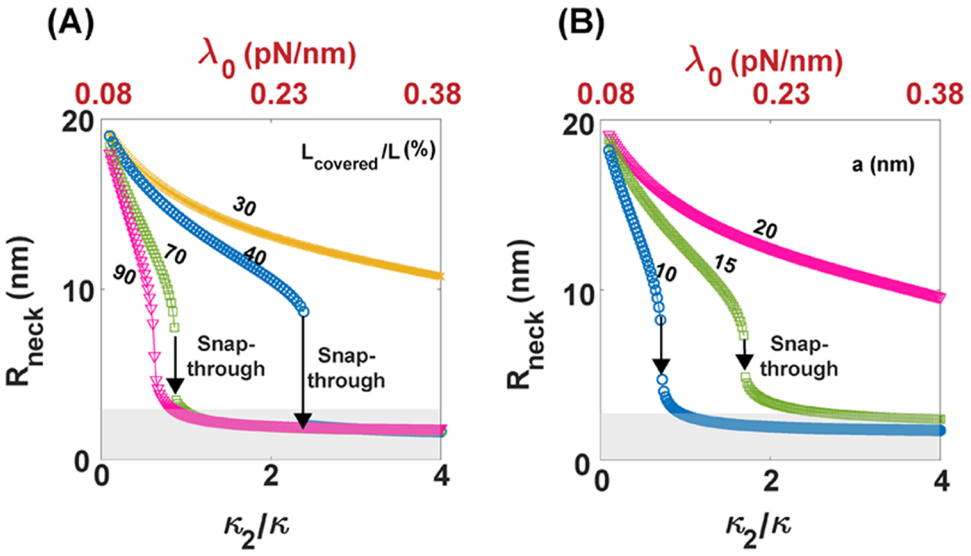

Figure 6. Membrane anisotropic bending rigidity coupled with tension controls the constriction of the mitochondrial fission neck through dynamin-induced deviatoric curvature. (A) The radius of the constricted mitochondrial neck as a function of the anisotropic to isotropic bending moduli ratio (k_2/k) for different protein coverages (a = 10 nm). We identified three distinct regimes. (I) For large protein coverage ($L_{covered}/L$ = 90%), the neck radius smoothly decreases into the hemi-fission regime as k_2/k increases. (II) For intermediate protein coverages (40% < $L_{covered}/L$ < 70%), there is a snap-through transition into the hemi-fission regime with increasing k_2/k. (III) For small protein coverage ($L_{covered}/L$ = 30%), the neck radius slightly decreases as k_2/k varies. The membrane tension at the boundary is set to be $\lambda_0 = (k + k_2)/4R_0^2$ and the corresponding boundary tension for each k_2/k value is marked at the top of the graph. (B) The radius of the constricted mitochondrial neck as a function of k_2/k for three different cubic lattice constants ($L_{covered}/L$ = 80%). For lattice constants of a = 10 and 15 nm, the transition into the spontaneous hemi-fission is associated with a snap-through instability. However, for a small lattice constant (a = 20 nm), the neck radius slightly decreases with an increase in k_2/k. In all simulations, we set the L/R_0 = 2.

Our results showed that the necks become narrower with increasing membrane bending rigidity, i.e., k_2/k, which is consistent with previous studies.[67,68] The comparison between the estimated neck radius from the analytical solution and the simulation results is shown in Figure S2. Interestingly, we observed three different dynamics of neck constriction, depending on the percentage of protein coverage. (i) For large protein coverage of $L_{covered}/L$ = 90%, the neck radius decreases smoothly as the bending moduli ratio increases, approaching the spontaneous hemi-fission limit at a k_2/k > 0.8 (pink line in Figure 6A). (ii) For a protein coverage of 40% < $L_{covered}/L$ < 70%, we observed a snap-through transition from a wide neck to a narrow neck below the hemi-fission threshold as the bending moduli ratio increased (green and blue lines in Figure 6A). Based on our results, the snap-through transition shifts to larger k_2/k ratio with decreasing the protein coverage (green and blue lines in Figure 6A). (iii) For a protein coverage of $L_{covered}/L$ = 30%, our results showed that the radius of the neck slightly decreases as the bending moduli ratio increases up to k_2/k = 4 (yellow line in Figure 6A).

We also plotted the radius of the neck as a function of the bending modulus ratio for three different cubic lattice constants (Figure 6B, $L_{covered}/L$ = 80%). We observed that, for small cubic lattice constants (a = 10 and 15 nm), the constriction of mitochondrial membrane with increasing the anisotropic bending rigidity, is associated with a snap-through instability (blue and green lines in Figure 6B). In contrast, for a large lattice constant (a = 20 nm), the radius of the neck slightly decreases as the bending rigidity ratio increases (pink line in Figure 6B). The anisotropic bending rigidity of the membrane characterizes the magnitude of the membrane tension as we set $\lambda_0 = (k + k_2)/4R_0^2$. Previous studies have demonstrated that membrane tension plays an important role in governing the efficiency of mitochondrial fission.[12,58,70−73] For example, in a low tension regime, complete fission occurs within a few minutes, while in a high membrane tension regime, it takes only a few seconds.[12,58,70−73] In Figure 6, the variation in k_2/k from 0 to 4 corresponds to a membrane tension varying from $\lambda_0 \sim 0.08$ to $\lambda_0 \sim 0.4$ pN/nm. Morlot et al. have experimentally shown that a high membrane tension, in the order of $\lambda_0 \sim$ O (0.1) pN/nm, is required for successful mitochondrial fission within a few seconds.[72] Thus, our results suggest that the dynamics of mitochondrial fission is governed by a complex interdependent relationship between membrane tension and the anisotropic bending rigidity of the membrane, covered by curvature-generating proteins.

Experimental Results Show Dynamin Family of Proteins Can Induce Mitochondrial Fission in a Cardiolipin-Dependent Manner. Having established a mechanical framework to estimate the size of constricted necks by the dynamin family of proteins from the cubic structures observed in SAXS experiments, it is interesting to compare the fission necks generated by Dnm1 and Drp1 in different lipid compositions. We have previously shown that Dnm1 can remodel lipid membranes to cubic structures with NGC.[25] To test the membrane deformations induced by Drp1, we incubated Drp1 with small unilamellar vesicles (SUVs) at a protein-to-lipid (P/L) molar ratio of 1/1000 (Figure 6A and Figure S3). The SUVs were prepared using two different ternary phospholipid compositions of phosphatidylethanolamine (PE), phosphatidylcholine (PC), and cardiolipin (CL) at molar ratios of 75/15/10 and 75/5/20 to mimic the lipid compositions of mitochondrial membranes.[74] We found that Drp1 restructured the lipid vesicles into an inverted hexagonal phase and a *Pn3m* cubic phase with a lattice constant of a = 19.075 and a = 34 nm for 75/5/20 and 75/15/10 PE/PC/CL,

https://doi.org/10.1021/jacs.5c06352
J. Am. Chem. Soc. XXXX, XXX, XXX−XXX

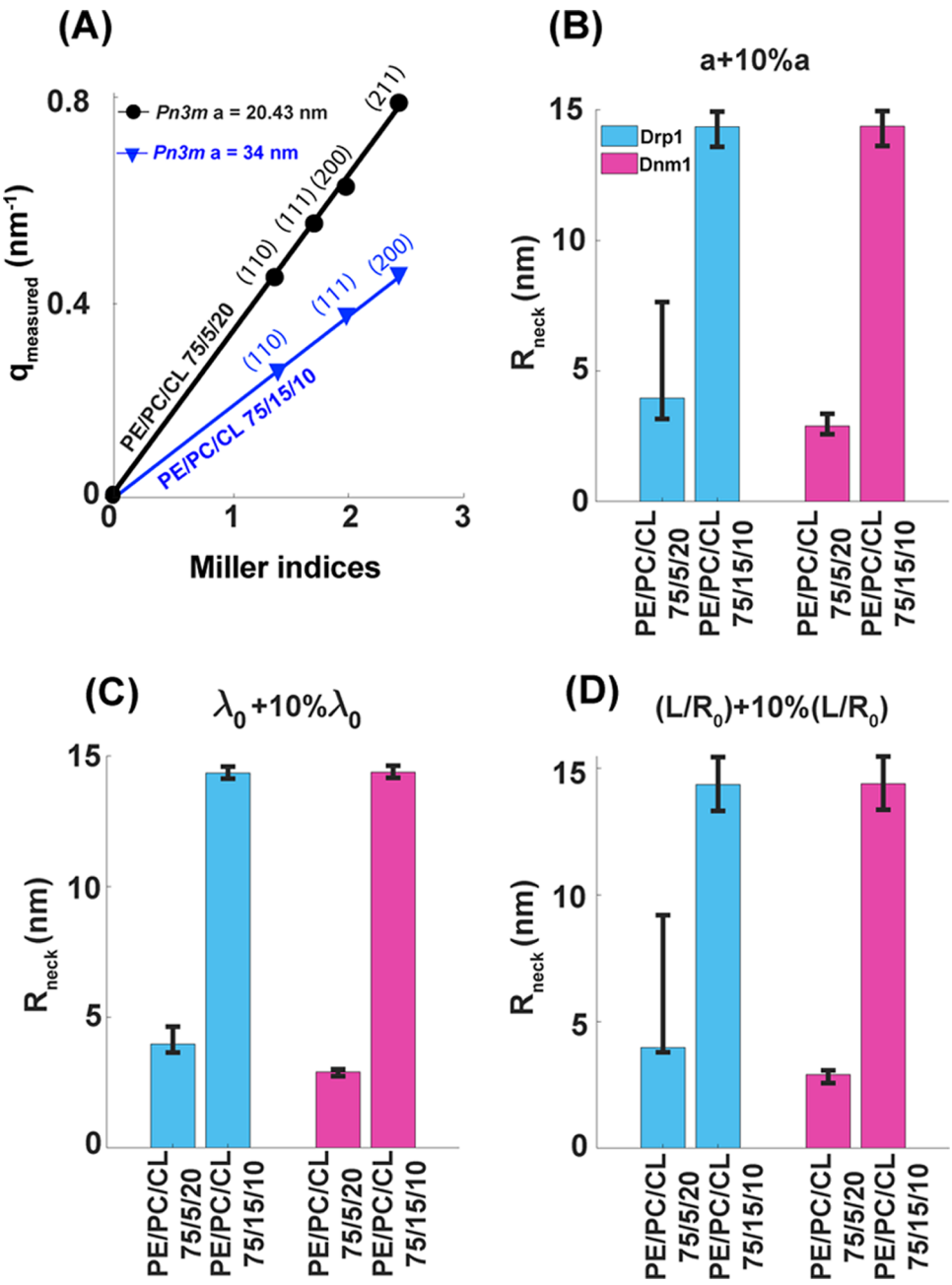

Figure 7. Variations in the size of scission necks induced by Drp1 and Dnm1 in two different lipid compositions. (A) Indexing of Drp1-induced cubic phases for 75/5/20 PE/PC/CL (black line) and 75/15/10 PE/PC/CL (blue line) model membranes at a protein-to-lipid (P/L) molar ratio of 1/1000. Plots of the measured q positions ($q_{measured}$) versus the assigned reflections are in terms of Miller indices. Estimated radius of the constricted neck, accounting for 10% variations in (B) cubic lattice constants, (C) membrane tension (λ_0 = 0.3 pN/nm), and (D) length of the tubular membrane (L/R_0 = 2). In all simulations, $L_{covered}/L$ = 99%.

respectively (Figure 7A and Figure S3). The hexagonal phase, having higher symmetry, produces more intense diffraction peaks, while the cubic phase, with lower symmetry, gives rise to a greater number of weaker peaks. In addition to symmetry considerations, the coexistence of these two phases is influenced by their distinct lipid composition requirements. The dominant lipid in our model membrane, PE, has a packing parameter $\left(\frac{\text{Volume}}{\text{Surface area} \times \text{length}}\right) \approx 1.2-1.3$, which favors negative Gaussian curvature. This suggests that PE-rich, phase-separated microdomains preferentially form inverted hexagonal phases, whereas mixed regions containing PE, PC, and CL stabilize cubic phases.

We next applied our framework to explore the degree of neck constriction by Dnm1 and Drp1 in different lipid compositions (Figure 7B–D). Using SAXS measurements as a baseline, we calculated the radius of constricted necks considering 10% variations in cubic lattice constants (representing technical variability), membrane tension (λ_0 = 0.3 pN/nm), and the length of the tubular membrane (L/R_0 = 2) (Figure 7B–D). We assumed high membrane tension in our calculations, based on experimental observations that typical mitochondrial fission rate over a few seconds, is associated with a high membrane tension regime.[72] We found that the efficiency of curvature-induced constriction highly depends on

https://doi.org/10.1021/jacs.5c06352
J. Am. Chem. Soc. XXXX, XXX, XXX−XXX

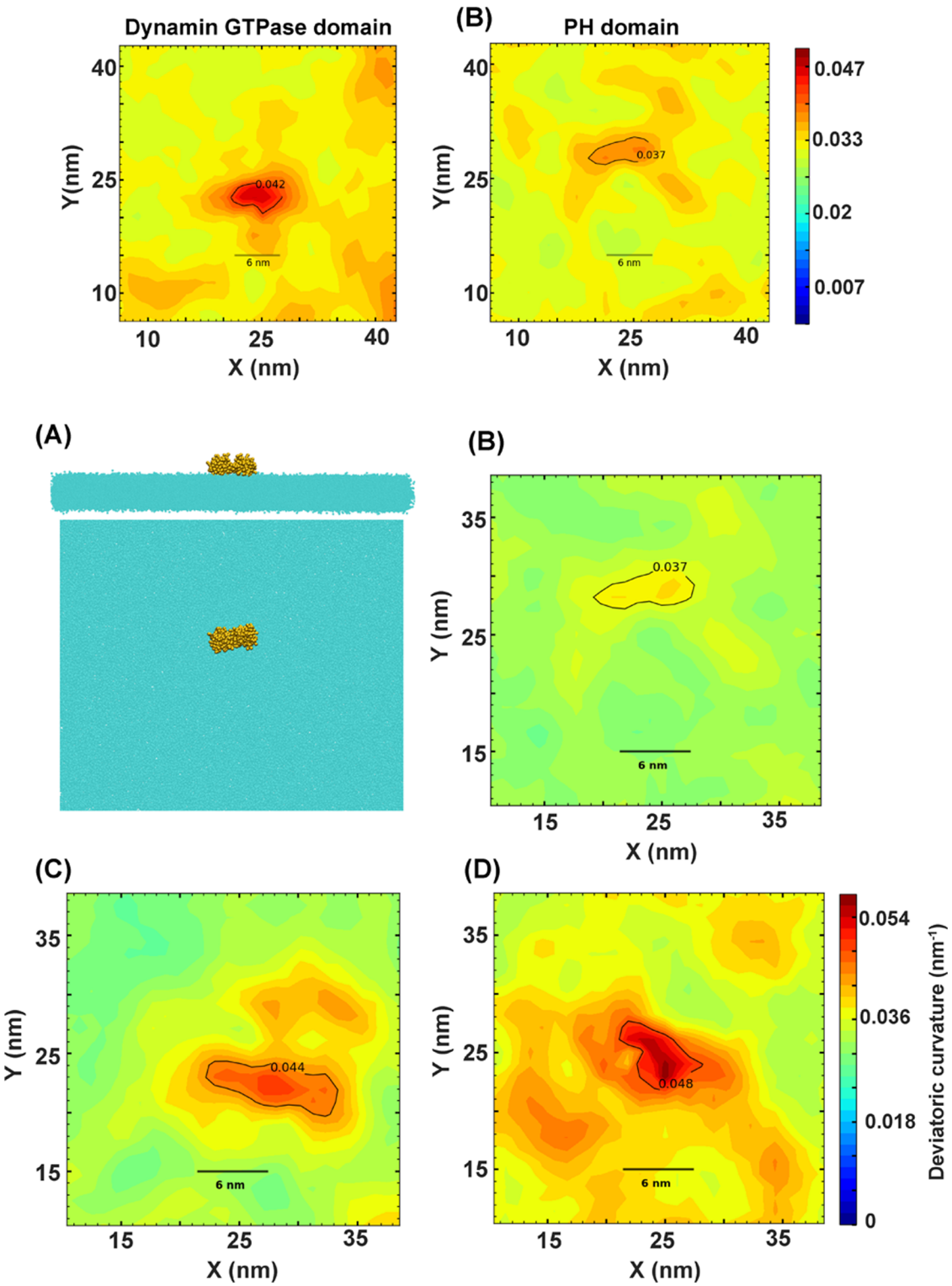

Figure 8. Comparison of the magnitude of deviatoric curvature induced by dynamin-like proteins with changing the protein coverage and the cardiolipin concentration of the lipid membrane using molecular dynamics simulations. (A) The snapshot shows the top and side views of the lipid membrane containing two IDVD domains. Deviatoric curvature was induced by (B) two and (C) four IDVD domains on a 75/15/10 PE/PC/CL lipid membrane. (D) Deviatoric curvature induced by two IDVD domains on a 75/5/20 PE/PC/CL membrane.

the composition of the mitochondrial membrane (Figure 7). Based on our results, in membranes with high cardiolipin concentration (PE/PC/CL 75/5/20), induced anisotropic curvature by Drp1 and Dnm1 can robustly constrict tubular membranes into narrow necks within the spontaneous hemifission range (Figure 7B–D). However, in membranes with low cardiolipin concentration, the induced curvature by Drp1 and Dnm1 slightly remodels membranes, forming wide necks with $R_{neck} \sim 15$ nm (Figure 7B–D).

Cardiolipin (CL) is an atypical, negatively charged, dimeric phospholipid that is predominantly enriched in the inner mitochondrial membrane, where it constitutes approximately

https://doi.org/10.1021/jacs.5c06352
J. Am. Chem. Soc. XXXX, XXX, XXX−XXX

20−25% of total lipids. In contrast, the outer mitochondrial membrane typically contains ∼3−10% CL under homeostatic conditions.[75] Previous studies have shown that CL plays a critical role in facilitating membrane−dynamin interactions and activating the GTPase domain of fission proteins.[26−28,76] For example, Macdonald et al. demonstrated that CL concentrations above 10% are required to promote robust Drp1 recruitment and GTPase activity in vitro using synthetic liposomes.[27] Similarly, Ugarte-Uribe et al. reported that higher CL levels (20−30%) are necessary for homogeneous Drp1 distribution and enhanced enzymatic activity.[77] To account for such high local CL concentrations at mitochondrial fission sites, previous studies have proposed mechanisms such as lipid redistribution at outer−inner membrane contact regions (e.g., ER−mitochondria junctions), as well as lipid phase separation driven by raft-promoting lipids.[26,75,78,79] These processes can locally enrich CL in the outer membrane, generating microdomains that serve as hotspots for mitochondrial membrane remodeling.[26,78,80]

Our estimated neck sizes induced by Drp1 and Dnm1 are ∼5× smaller than the diameters of constricted lipid tubules observed by electron microscopy for lipid-bound Drp1 oligomerization with 100% phosphatidylserine (PS) lipid composition.[81,82] This could be due to the synergetic effects of lipid composition, mutually amplifying mechanical fission forces from membrane remodeling proteins, and Drp1 adaptors/recruiters that are responsible for bringing Drp1 to the specific sites of fission. In particular, CL is a canonical lipid with intrinsic negative spontaneous curvature which localizes to concave membrane regions and reduces bilayer rigidity.[83] This CL-induced negative spontaneous curvature ($C_0 < 0$) lowers the bilayer Gaussian modulus ($\kappa_{G,bilayer} = 2(\kappa_{monolayer} - 2\kappa_{monolayer}C_0z_0)$),[84] thereby decreasing the energetic cost of topological transitions[85] required for neck formation during mitochondrial fission. Consistently, our results suggest that a modest reduction in the percentage of CL in lipid composition from 20% to 10% results in a nearly 5× increase in the radius of the scission neck induced by Drp1 and Dnm1 (Figure 7), which can potentially make successful hemi-fission statistically improbable. Additionally, we observed that in membranes with high cardiolipin concentration, the radius of the constricted neck shows greater variability in response to changes in system properties, compared to compositions with lower cardiolipin concentration (Figure 7). This can be an indication of the stochastic characteristic of the hemi-fission reaction, as suggested by both in *vivo* and in *vitro* experiments.[20,86−88]

Coarse-Grained Molecular Dynamics Simulations Show Larger Protein Coverage Induces Stronger Deviatoric Curvature and Its Strength Depends on Membrane Cardiolipin Concentration. Our results from the continuum framework and SAXS data suggest that the dynamin family of proteins can constrict fission necks by imposing anisotropic curvature on the underlying tubular membrane. Based on our findings, the degree of anisotropic curvature generated by the dynamin family of proteins depends on the extent of membrane coverage by the protein (Figure 3) and the percentage of cardiolipin in the lipid membrane (Figure 7). To test this hypothesis, we conducted coarse-grained molecular dynamics simulations with the IDVD domains of Dnm1 on two different membrane lipid compositions: 75/5/20 PE/PC/CL and 75/15/10 PE/PC/CL (Figure 8). In the first simulations, we placed two IDVD domains of Dnm1 on a 75/15/10 PE/PC/CL membrane in such a way that the variable loops are closer to the membrane surface (Figure 8A). The system was equilibrated for 2 μs, and the equilibrated trajectory was used to compute the deviatoric curvature generated on the membrane. Details of the simulation protocol and calculations of deviatoric curvature are described in the Supporting Information. Figure 8B shows that the IDVD domain of Dnm1 can generate a deviatoric curvature on the membrane surface. We then increased the protein coverage on the membrane (corresponding to the $L_{covered}$ of the theoretical model) by placing four IDVD domains on the membrane surface and observed an ∼19% increase in the magnitude of induced deviatoric curvature on the membrane surface (Figure 8C). This is consistent with the prediction of our theoretical model that a larger protein coverage induces narrower mitochondrial fission necks (Figure 3A).

Next, we investigated the effect of lipid composition, particularly cardiolipin, on the degree of deviator curvature generated by Dnm1. We placed two IDVD domains on the surface of a 75/5/20 PE/PC/CL lipid membrane (Figure 8D). Our results show that the deviatoric curvature induced by Dnm1 on this lipid membrane is significantly (∼30%) higher than the deviatoric curvature generated on a 75/15/10 PE/PC/CL lipid membrane (Figure 8B,D). This is also in agreement with our theoretical predictions and SAXS experiments, which show that a modest increase in the percentage of cardiolipin in the lipid composition results in a significant decrease in the radius of the scission neck induced by Dnm1 proteins. Additionally, we observed that the induced deviatoric curvature on the 75/5/20 PE/PC/CL lipid membrane extends to a relatively larger distance compared to that on the 75/15/10 PE/PC/CL lipid membrane (Figure 8B,D), which might be due to increased membrane fluidity with increasing cardiolipin concentration.[89] A previous study has suggested that the mechanical stability of lipid membranes decreases with increasing cardiolipin concentration.[89] This implies that a higher concentration of cardiolipin in the mitochondrial membrane can facilitate the process of fission neck constriction, as predicted by our coarse-grained simulations and theoretical model.

Mitochondria are dynamic organelles that constantly undergo fission and fusion processes. The balance between these two processes plays an important role in modulating the shape, distribution of mitochondria, and bioenergetics.[1−3] For example, excessive fission of mitochondria has been implicated in neurodegenerative diseases.[4−6] The dynamin family of proteins (Dnm1 in yeast and its conserved human homologues, Drp1) is key molecular machinery responsible for regulating mitochondrial fission.[1,7−10] Despite three decades of experimental work, the mechanical principle underlying membrane scission is still unclear.[12] Dynamin is a mechanochemical enzyme, and current models for dynamin-driven fission can broadly be categorized into two main classes: (I) the two-step model and (II) the constrictase model.[12] In the two-step model, helical assembly of dynamin-like proteins first slowly constricts the mitochondrial membrane into a tubular structure, followed by a rapid transition to scission, driven by GTP hydrolysis-induced oligomer disassembly.[12,17−19] However, this process requires high cooperativity among dimers, which is inconsistent with the low measured Hill coefficient, and the suggests disassembly could cause tubule widening due to the slower rate of dynamin disassembly compared to membrane viscoelasticity. On the other hand, in the

https://doi.org/10.1021/jacs.5c06352
J. Am. Chem. Soc. XXXX, XXX, XXX−XXX

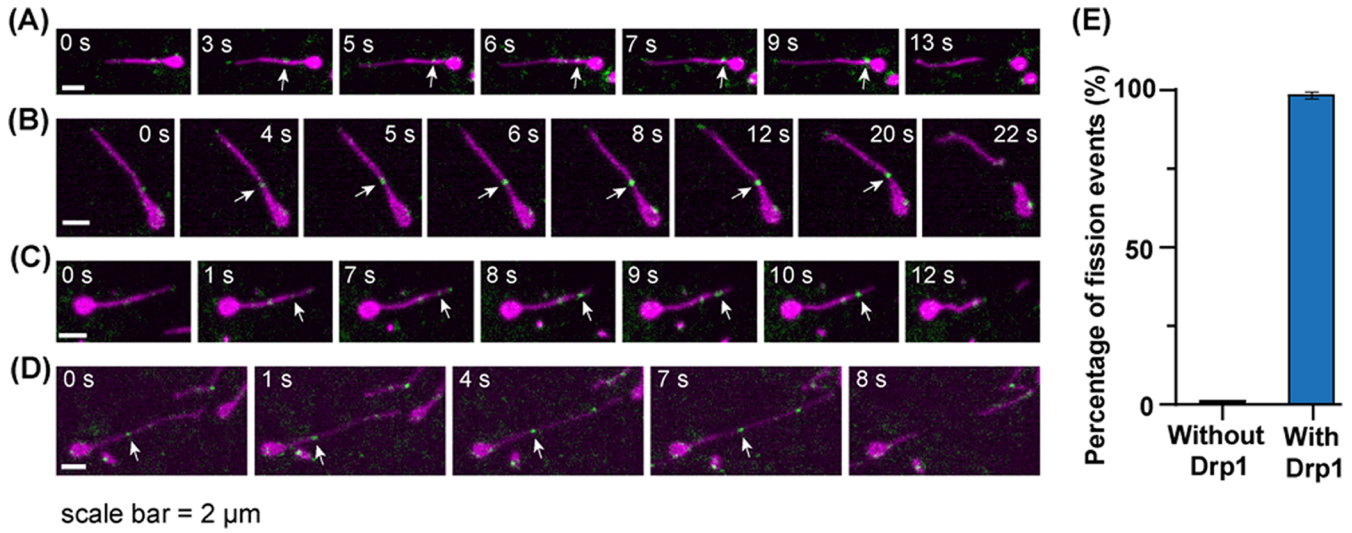

Figure 9. Drp1 facilitates complete fission on the constricted mitochondrial membrane. (A–D) Fluorescence images of COS-7 cells transfected with iLID-tdTomato-omp25 (magenta), KIF5A-SspB, and GFP-Drp1 (green). Arrows indicate Drp1 puncta on the mitochondria. (A and B) Fission occurs at the junction between the mitochondrial body and the extended outer mitochondria membrane. (C and D) Fission occurs in the middle of the confined outer mitochondria membrane. (E) The percentage of mitochondrial fission occurring in the presence or absence of Drp1 puncta at fission sites. 407 fission events from 6 independent experiments were quantified. Scale bars, 2 μm.

constrictase model, dynamin-like proteins serve as a molecular motor protein where GTP hydrolysis prompts the sliding of helices, leading to spontaneous hemi-fission. However, in this model, how disassembly occurs and how such disassembly contributes to scission remain a matter of debate. In particular, the required number of interacting helicoidal coils to generate the force necessary for scission seems to be variable, exhibiting a degree of stochasticity. These open challenges in each dynamin fission model are further complicated by the extreme changes in the geometry of the mitochondrial membrane during the fission process, transitioning from a tubular structure to a catenoid-shaped neck with a large NGC.

Our results from the mechanical framework combined with SAXS measurements suggest that the fission protein machinery of dynamin governs mitochondrial fission through both its helix-driven mechanical confinement of the tubular membrane and its synergistic curvature-driven snap-through instability. A previous study by Irajizad et al. suggested that actin-and Drp1-mediated forces, combined with the curvature induced by conical lipids localized in the pinching domain, can trigger buckling instability during mitochondrial fission.[23] Here, we propose that the NGC induced by dynamin-like proteins alone is sufficient to drive the snap-through instability and generate superconstricted fission necks below the membrane's hemi-fission threshold. It is interesting to note that our machine learning analysis shows that the strongest NGC-inducing domain in Dnm1 is not the variable domain facing the confined membrane tubule, but rather the GTPase domain more distal from it.[25] In support of this, we showed in the companion paper[90] that the hydrolysis-driven oligomer disassembly and concomitant creation of a population of mobile dynamins can significantly amplify NGC generation by presentation of the free NGC-generating GTPase domain in the vicinity of the mitochondrion.

Direct manipulation of mitochondrial scission in cells has been historically difficult. To further test our hypothesis that long thin mitochondrial tubes can be forced to undergo scission via interaction with NGC-generating Drp1, we have to devise a way to separate the process of getting to the initial condition of confined tube formation from the process of induced scission. To accomplish that, we conducted *in vitro* experiments and time-course live-cell imaging of mitochondria (Figure 9). To form narrow membrane tubes (diameter <300 nm), we employed an optogenetic mechanostimulation system to apply tensile forces to mitochondria in live COS-7 cells.[91,92] This system utilized the optical dimerizer iLID, fused to tdTomato and OMP25 to target the outer mitochondrial membrane, along with a truncated, cargo-binding-deficient kinesin (KIF5A) fused to SspB. Upon blue light stimulation, iLID–SspB binding occurred within seconds, recruiting kinesin motors to the outer mitochondrial membrane (shown in magenta) and generating pulling forces that induced the formation of thin mitochondrial tubules with pronounced curvature (Figure 9). Using this system, we observed that GFP-tagged Drp1 puncta (shown in green) dynamically assembled at constriction sites prior to fission—either at tubule-body junctions or along thin tubules characterized by nonpositive Gaussian curvature. These sites minimize elastic energy mismatch,[39] thereby facilitating the final step of mitochondrial fission (Figure 9A–D). Analysis of 407 fission events revealed that 96% ± 1% were preceded by localized Drp1 enrichment at the future fission site (Figure 9E), indicating that curvature-sensitive Drp1 recruitment plays a critical role in facilitating mechanically induced mitochondrial division.

Previous studies have proposed the presence of mechanical instability during dynamin constriction due to an increase in the helical pitch of the dynamin assembly or an adjustment in the spontaneous curvature of the neck membrane to favor negative values.[93,94] Our results introduce a new perspective; the collar pressure induced by helical assemblies of dynamin-like proteins smoothly constricts the mitochondrial membrane into narrow necks (Figure 4), while curvature-driven remodeling is associated with a snap-through transition (Figure 3). This difference resembles the observed dynamics of slow and smooth membrane neck constriction facilitated by

https://doi.org/10.1021/jacs.5c06352
J. Am. Chem. Soc. XXXX, XXX, XXX–XXX

assembly of dynamin-like proteins, followed by the fast mitochondrial fission step after GTP hydrolysis, which induces helix disassembly, a phenomenon broadly observed experimentally. These effects essentially recapitulate the major observed features of the two-step model of dynamin-induced mitochondrial fission. It should be noted that our focus here was on the equilibrium shapes of the membrane, and we did not model the exact dynamic transitions between stages. However, from a mechanical perspective, we can expect that the curvature-induced "snap-through" transition to occur within the membrane relaxation time scale (∼ms),[95,96] which is comparable to experimental observations for the fast induced fission by dynamin disassembly in the two-step model.[12] It should be noted that our focus here was on the equilibrium shapes of the membrane, and we did not model the exact dynamical transitions between stages. However, from a mechanical perspective, we can expect that the curvature-induced "snap-through" transition to occur within the membrane relaxation time scale (∼ms),[95,96] which is comparable to experimental observations for the fast induced fission by dynamin disassembly in the two-step model.[12]

Importantly, we find that longer tubular membranes (length/ratius >1.8) are more prone to undergoing the fission process in response to the NGC generated by the dynamin family of proteins (Figure 5). Our results demonstrate that, under a large induced NGC, a snap-through transition occurs in the hemi-fission region as the length of a tubular membrane increases (Figure 5). This length-associated snap-through instability may serve as the driving mechanism for spontaneous hemi-fission in the constrictase model, considering that the tubular membrane elongates with constriction.[62] What is more, our results here suggest that there is an intrinsic stochasticity to the fission process, since in principle different combinations of dynamin helical oligomer confinement, free dynamin mediated membrane remodeling, and membrane tubule length can lead to completion of fission. Taken together, our model predicts that if there is a disruption in either (1) oligomerization of dynamin-like proteins and the formation of confined narrow tubules or (2) curvature-driven remodeling, the wide membrane tube would fail to undergo fission, and the process would be inhibited. For example, a recent study by K. Rochon et al. demonstrated that Drp1 adopts an autoinhibited dimer conformation, in which the GTPase domain is locked against the stalk via interactions with the BSE and loop L3S, preventing higher-order oligomerization and ultimately membrane fission.[97] Consistent with our model, a lack of membrane-bound oligomerization results in the formation of wide membrane tubules in which the induced NGC by free dynamin-like proteins is insufficient to drive fission. Additionally, in vitro experiments by B. Ugarte-Uribe et al. using recombinant human Drp1 and mitochondria-like lipid compositions demonstrated that Drp1 polymerization stabilizes tubular membranes without inducing fission.[77] This finding aligns with our model prediction and the results from the companion paper,[90] suggesting that Drp1 disassembly and the free Drp1 subunits are required to position the NGC-generating GTPase domain near the mitochondrial membrane to promote fission. However, future studies are needed to elucidate the precise mechanisms of dynamin-induced fission and the role of protein disassembly combined with adaptor proteins and dynamin 2 in mediating the final step of mitochondrial division.

Currently, the precise number of dynamin helical turns required to induce mitochondrial fission is not so clear.[12] Based on our results, a purely compressive mechanism requires a collar pressure >75 pN/nm to form narrow necks (R_{neck} < 3 nm), below the spontaneous hemi-fission limit. Using electron microscopy and Hooke's law, Stowell et al.[62] initially estimated that each helical turn of dynamin can exert a compressive force of approximately 110 pN. However, using micropipette−optical tweezer, Roux et al. later estimated that each helical turn generates significantly lower compressive forces, on the order of ∼20 pN.[98] Considering the helical pitch of dynamin (∼13 nm), the distinct force estimates reported by Stowell et al. and Roux et al. lead to different predictions regarding the number of helical turns required to generate the necessary collar pressure. Notably, these predictions contrast with *in vivo* findings, where even a single helical turn may be sufficient for mitochondrial fission.[88,99] Taken together, these observations suggest that dynamin likely operates through a combination of mechanical constriction and curvature-driven membrane remodeling, which forms the core of our proposed model in this study.

We believe that the results presented here represent an important step toward deciphering the intricate mechano-chemical principles underlying mitochondrial fission. Our findings can be a motivation for future studies to develop quantitative relationships between GTP-driven disassembly of dynamin and the generation of membrane-destabilizing curvature. In particular, in the companion paper,[90] we elucidate how dynamin-like proteins mediate fission across a heterogeneously uncorrelated population in response to varying levels of GTP hydrolysis. This could provide valuable insights into the relationship between GTP-driven disassembly and membrane scission as well as the precise role of energy derived from GTP hydrolysis in enabling dynamin-mediated mitochondrial fission. Beyond mitochondrial fission, classical dynamins (dynamins 1, 2, and 3) are known to regulate membrane scission during endocytosis. These proteins contain a pleckstrin homology (PH) domain that mediates their interaction with lipid membranes, particularly binding to phosphatidylinositol (4,5)-bisphosphate (PI(4,5)P2). It has been proposed that dynamins play dual roles in endocytosis: (1) promoting early membrane invagination through the GTPase-like activity of unassembled dynamin and (2) self-assembling and constricting lipid necks via GTP hydrolysis.[100] Different mechanical models—from pinchase model to induced fission by shear and depolymerization—have been proposed to explain how dynamin induces membrane fission.[101] Future studies are needed to investigate the capacity of free (nonassembled) dynamins to form membrane invaginations—dome-shaped structures with positive Gaussian curvature (Figure 2A)—and to induce compressive stresses, in combination with membrane tension and twist, to drive fission.

Despite the agreement between our model predictions and experimental observations, we acknowledge some limitations and simplifying assumptions in our current framework. Specifically, we model the mitochondrial membrane as a single lipid bilayer with a rotationally symmetrical tubular geometry. In reality, mitochondrial membranes are more complex: they consist of a double bilayer structure (inner and outer membranes), and their geometry is not necessarily axisymmetric. As a first approximation, the overall effect of the double membrane can be incorporated by defining an effective bending modulus as the sum of the contributions from both

https://doi.org/10.1021/jacs.5c06352
J. Am. Chem. Soc. XXXX, XXX, XXX−XXX

bilayers ($\kappa_{eff} = \kappa_{outer\ membrane} + \kappa_{inner\ membrane}$). Altering the magnitude of the bending rigidity does not affect our results for curvature-driven constriction and the snap-through transition (Figures 3 and 5−7), since bending rigidity and the set membrane tension at the boundary are coupled to maintain the tubular membrane geometry ($\lambda_0 = \lambda_{cylinder} = (\kappa + \kappa_2)/4R_0^2$). However, higher compressive forces are required to achieve membrane constriction with increased bending rigidity (Figure 4). Ultimately, future work will aim to extend the model to explicitly incorporate double bilayer membranes and fully 3D geometries without symmetry constraints. Such advancements are critical for accurately capturing the mechanics of outer membrane constriction and the potential coupling between the inner and outer membranes during mitochondrial fission. For example, a recent study by X. Liu et al. demonstrated that it is possible for the outer mitochondrial membrane to separate from the inner membrane during tubulation and force-induced tail-autotomy mitochondrial fission.[92] Additionally, in our current framework, we model the effects of dynamin helical assembly and GTP hydrolysis at a high level—as a compressive stress that constricts the tubular membrane—without explicitly incorporating the biochemical GTPase cycle of dynamins. Future extensions of this framework are needed to include GTPase dynamics to quantitatively capture the coupling between the chemical energy input and the mechanical response of the membrane.

METHODS

The complete derivations with details are given in the Supporting Information.

ASSOCIATED CONTENT

Supporting Information

The Supporting Information is available free of charge at https://pubs.acs.org/doi/10.1021/jacs.5c06352.

Complete derivations with details; Supplemental Figure S1 shows the radius of the constricted neck by curvature inducing proteins as the function of tubule height, Supplemental Figure S2 demonstrates the radius of the constricted neck as the function of anisotropic to isotropic bending rigidity ratio, and Figure S3 is the SAXS spectra induced by Drp1 on two different lipid membrane compositions (PDF)

AUTHOR INFORMATION

Corresponding Author

Gerard C. L. Wong − *Department of Bioengineering, University of California, Los Angeles, Los Angeles, California 90025, United States; Department of Chemistry and Biochemistry, Department of Microbiology, Immunology, and Molecular Genetics, and California NanoSystems Institute, University of California, Los Angeles, California 90095, United States;* orcid.org/0000-0003-0893-6383; Email: gclwong@seas.ucla.edu

Authors

Haleh Alimohamadi − *Department of Bioengineering, University of California, Los Angeles, Los Angeles, California 90025, United States; Department of Chemistry and Biochemistry, Department of Microbiology, Immunology, and Molecular Genetics, and California NanoSystems Institute, University of California, Los Angeles, California 90095, United States;* orcid.org/0000-0001-6576-2426

Elizabeth Wei-Chia Luo − *Department of Bioengineering, University of California, Los Angeles, Los Angeles, California 90025, United States; Department of Chemistry and Biochemistry, Department of Microbiology, Immunology, and Molecular Genetics, and California NanoSystems Institute, University of California, Los Angeles, California 90095, United States;* orcid.org/0000-0002-8663-0446

Xiaoying Liu − *Department of Biomedical Engineering, The Chinese University of Hong Kong, Hong Kong, Sha Tin, China*

Wasi Iqbal − *Department of Biomedical Engineering, The Chinese University of Hong Kong, Hong Kong, Sha Tin, China*

Rena Yang − *Department of Bioengineering, University of California, Los Angeles, Los Angeles, California 90025, United States; Department of Chemistry and Biochemistry, Department of Microbiology, Immunology, and Molecular Genetics, and California NanoSystems Institute, University of California, Los Angeles, California 90095, United States*

Shivam Gupta − *Department of Physics, Indian Institute of Technology Kanpur, Kanpur 208016, India;* orcid.org/0009-0003-7256-434X

Kelsey A Nolden − *Department of Biochemistry, Medical College of Wisconsin, Milwaukee, Wisconsin 53226, United States*

Taraknath Mandal − *Department of Physics, Indian Institute of Technology Kanpur, Kanpur 208016, India;* orcid.org/0000-0002-9902-2415

R. Blake Hill − *Department of Biochemistry, Medical College of Wisconsin, Milwaukee, Wisconsin 53226, United States; Department of Pharmaceutical Sciences, University of Colorado, Anschutz Medical Campus, Aurora, Colorado 80045, United States*

Liting Duan − *Department of Biomedical Engineering, The Chinese University of Hong Kong, Hong Kong, Sha Tin, China*

Complete contact information is available at: https://pubs.acs.org/10.1021/jacs.5c06352

Notes

The authors declare no competing financial interest.

ACKNOWLEDGMENTS

This work was supported by American Heart Association AHA966662 grant and NSF DMR2325840 (G.C.L.W.), National Institutes of Health grant R01GM067180 (R.B.H., G.C.L.W.), and Vascular Biology Training Grant T32 HL069766-21 (H.A). T.M. gratefully acknowledges the support from the Government of India: Science and Engineering Research Board via Sanction No. SRG/2022/000548. We thank the Stanford Synchrotron Radiation Lightsource (SSRL) (Menlo Park, CA, USA) for access to beamline 4-2. Use of the SSRL, SLAC National Accelerator Laboratory, is supported by the U.S. Department of Energy, Office of Science, Office of Basic Energy Sciences under contract no. DE-AC02-76SF00515. The SSRL Structural Molecular Biology Program is supported by the U.S. Department of Energy, Office of Biological and Environmental Research, and by the National Institutes of Health, National Institute of General Medical Sciences (including P30GM133894). T.M. is grateful for the computational resources provided by PARAM Sanganak under

the National Supercomputing Mission, Government of India, at the Indian Institute of Technology, Kanpur.

REFERENCES

(1) Bleazard, W.; et al. The dynamin-related GTPase Dnm1 regulates mitochondrial fission in yeast. *Nat. Cell Biol.* **1999**, *1*, 298−304.
(2) Westermann, B. Mitochondrial fusion and fission in cell life and death. *Nat. Rev. Mol. Cell Biol.* **2010**, *11*, 872−884.
(3) Sesaki, H.; Jensen, R. E. Division versus Fusion: Dnm1p and Fzo1p Antagonistically Regulate Mitochondrial Shape. *J. Cell Biol.* **1999**, *147*, 699−706.
(4) Benarroch, E. What Is the Role of Mitochondrial Fission in Neurologic Disease? *Neurology* **2022**, *98*, 662−668.
(5) Yang, D. Mitochondrial Dynamics: A Key Role in Neurodegeneration and a Potential Target for Neurodegenerative Disease. *Frontiers in Neuroscience* **2021**, *15*, 654785.
(6) Archer, S. L. Mitochondrial Dynamics — Mitochondrial Fission and Fusion in Human Diseases. *New England Journal of Medicine* **2013**, *369*, 2236−2251.
(7) Shaw, J. M.; Nunnari, J. Mitochondrial dynamics and division in budding yeast. *Trends Cell Biol.* **2002**, *12*, 178−184.
(8) Smirnova, E.; Shurland, D. L.; Ryazantsev, S. N.; van der Bliek, A. M. A human dynamin-related protein controls the distribution of mitochondria. *J. Cell Biol.* **1998**, *143*, 351−358.
(9) Smirnova, E.; Griparic, L.; Shurland, D. L.; van der Bliek, A. M. Dynamin-related protein Drp1 is required for mitochondrial division in mammalian cells. *Mol. Biol. Cell* **2001**, *12*, 2245−2256.
(10) Otsuga, D.; et al. The dynamin-related GTPase, Dnm1p, controls mitochondrial morphology in yeast. *J. Cell Biol.* **1998**, *143*, 333−349.
(11) Jimah, J. R.; Hinshaw, J. E. Structural Insights into the Mechanism of Dynamin Superfamily Proteins. *Trends Cell Biol.* **2019**, *29*, 257−273.
(12) Antonny, B.; et al. Membrane fission by dynamin: what we know and what we need to know. *EMBO J.* **2016**, *35*, 2270−2284.
(13) Sweitzer, S. M.; Hinshaw, J. E. Dynamin Undergoes a GTP-Dependent Conformational Change Causing Vesiculation. *Cell* **1998**, *93*, 1021−1029.
(14) Chen, Y.-J.; Zhang, P.; Egelman, E. H.; Hinshaw, J. E. The stalk region of dynamin drives the constriction of dynamin tubes. *Nat. Struct Mol. Biol.* **2004**, *11*, 574−575.
(15) Fröhlich, C.; et al. Structural insights into oligomerization and mitochondrial remodelling of dynamin 1-like protein. *EMBO Journal* **2013**, *32*, 1280−1292.
(16) Mears, J. A.; et al. Conformational changes in Dnm1 support a contractile mechanism for mitochondrial fission. *Nat. Struct Mol. Biol.* **2011**, *18*, 20−26.
(17) Warnock, D. E.; Hinshaw, J. E.; Schmid, S. L. Dynamin Self-assembly Stimulates Its GTPase Activity *. *J. Biol. Chem.* **1996**, *271*, 22310−22314.
(18) Marks, B.; et al. GTPase activity of dynamin and resulting conformation change are essential for endocytosis. *Nature* **2001**, *410*, 231−235.
(19) Danino, D.; Moon, K.-H.; Hinshaw, J. E. Rapid constriction of lipid bilayers by the mechanochemical enzyme dynamin. *J. Struct. Biol.* **2004**, *147*, 259−267.
(20) Mattila, J.-P.; et al. A hemi-fission intermediate links two mechanistically distinct stages of membrane fission. *Nature* **2015**, *524*, 109−113.
(21) Vasan, R.; Rudraraju, S.; Akamatsu, M.; Garikipati, K.; Rangamani, P. A mechanical model reveals that non-axisymmetric buckling lowers the energy barrier associated with membrane neck constriction. *Soft Matter* **2020**, *16*, 784−797.
(22) Pannuzzo, M.; McDargh, Z. A; Deserno, M. The role of scaffold reshaping and disassembly in dynamin driven membrane fission. *eLife* **2018**, *7*, e39441.
(23) Irajizad, E.; Ramachandran, R.; Agrawal, A. Geometric instability catalyzes mitochondrial fission. *Mol. Biol. Cell* **2019**, *30*, 160−168.
(24) Frolov, V. A.; Lizunov, V. A.; Dunina-Barkovskaya, A. Y.; Samsonov, A. V.; Zimmerberg, J. Shape bistability of a membrane neck: a toggle switch to control vesicle content release. *Proc. Natl. Acad. Sci. U. S. A.* **2003**, *100*, 8698−8703.
(25) Lee, M. W.; et al. Molecular Motor Dnm1 Synergistically Induces Membrane Curvature To Facilitate Mitochondrial Fission. *ACS Cent. Sci.* **2017**, *3*, 1156−1167.
(26) Stepanyants, N.; et al. Cardiolipin's propensity for phase transition and its reorganization by dynamin-related protein 1 form a basis for mitochondrial membrane fission. *Mol. Biol. Cell* **2015**, *26*, 3104−3116.
(27) Macdonald, P. J.; et al. A dimeric equilibrium intermediate nucleates Drp1 reassembly on mitochondrial membranes for fission. *Mol. Biol. Cell* **2014**, *25*, 1905−1915.
(28) Joshi, A. S.; Thompson, M. N.; Fei, N.; Hüttemann, M.; Greenberg, M. L. Cardiolipin and mitochondrial phosphatidylethanolamine have overlapping functions in mitochondrial fusion in Saccharomyces cerevisiae. *J. Biol. Chem.* **2012**, *287*, 17589−17597.
(29) Helfrich, W. Elastic properties of lipid bilayers: theory and possible experiments. *Z. Naturforsch C* **1973**, *28*, 693−703.
(30) Deuling, H. J.; Helfrich, W. The curvature elasticity of fluid membranes: A catalogue of vesicle shapes. *J. Phys. (Paris)* **1976**, *37*, 1335−1345.
(31) Alimohamadi, H.; Rangamani, P. Modeling Membrane Curvature Generation due to Membrane−Protein Interactions. *Biomolecules* **2018**, *8*, 120.
(32) Alimohamadi, H. *Application of Continuum Mechanics for a Variety of Curvature Generation Phenomena in Cell Biophysics*; University of California: San Diego, 2021.
(33) Iglič, A.; Babnik, B.; Gimsa, U.; Kralj-Iglič, V. On the role of membrane anisotropy in the beading transition of undulated tubular membrane structures. *J. Phys. A: Math. Gen.* **2005**, *38*, 8527−8536.
(34) Alimohamadi, H.; Bell, M. K.; Halpain, S.; Rangamani, P. Mechanical principles governing the shapes of dendritic spines. *Frontiers in Physiology* **2021**, *12*, 657074.
(35) Kabaso, D.; et al. Attachment of Rod-Like (BAR) Proteins and Membrane Shape. *Mini Rev. Med. Chem.* **2011**, *11*, 272−282.
(36) Bobrovska, N.; Góźdź, W.; Kralj-Iglič, V.; Iglič, A. On the role of anisotropy of membrane components in formation and stabilization of tubular structures in multicomponent membranes. *PLoS One* **2013**, *8*, No. e73941.
(37) Walani, N.; Torres, J.; Agrawal, A. Anisotropic spontaneous curvatures in lipid membranes. *Phys. Rev. E Stat Nonlin Soft Matter Phys.* **2014**, *89*, 062715.
(38) Alimohamadi, H.; Rangamani, P. Effective cell membrane tension protects red blood cells against malaria invasion. *PLOS Computational Biology* **2023**, *19*, No. e1011694.
(39) Iglič, A.; Hägerstrand, H.; Veranič, P.; Plemenitaš, A.; Kralj-Iglič, V. Curvature-induced accumulation of anisotropic membrane components and raft formation in cylindrical membrane protrusions. *J. Theor. Biol.* **2006**, *240*, 368−373.
(40) Kabaso, D.; et al. On the role of membrane anisotropy and BAR proteins in the stability of tubular membrane structures. *J. Biomech* **2012**, *45*, 231−238.
(41) Iglic, A.; et al. On the role of anisotropy of membrane constituents in formation of a membrane neck during budding of a multicomponent membrane. *J. Biomech* **2007**, *40*, 579−585.
(42) Alimohamadi, H.; Vasan, R.; Hassinger, J.; Stachowiak, J.; Rangamani, P. The role of traction in membrane curvature generation. *Biophys. J.* **2018**, *114*, 600a.
(43) Mahapatra, A.; Rangamani, P. Formation of protein-mediated bilayer tubes is governed by a snapthrough transition. *Soft Matter* **2023**, *19*, 4345−4359.
(44) Yuan, F.; et al. Membrane bending by protein phase separation. *Proc. Natl. Acad. Sci. U.S.A.* **2021**, *118*, No. e2017435118.

https://doi.org/10.1021/jacs.5c06352
J. Am. Chem. Soc. XXXX, XXX, XXX−XXX

(45) Alimohamadi, H.; et al. How Cell-Penetrating Peptides Behave Differently from Pore-Forming Peptides: Structure and Stability of Induced Transmembrane Pores. *J. Am. Chem. Soc.* **2023**, *145*, 26095.
(46) Alimohamadi, H.; et al. Comparing Multifunctional Viral and Eukaryotic Proteins for Generating Scission Necks in Membranes. *ACS Nano* **2024**, *18*, 15545−15556.
(47) Harper, P. E.; Gruner, S. M. Electron density modeling and reconstruction of infinite periodic minimal surfaces (IPMS) based phases in lipid-water systems. I. Modeling IPMS-based phases. *Eur. Phys. J. E* **2000**, *2*, 217−228.
(48) Schwarz, U. S.; Gompper, G. Systematic approach to bicontinuous cubic phases in ternary amphiphilic systems. *Phys. Rev. E* **1999**, *59*, 5528−5541.
(49) Alimohamadi, H.; Smith, A. S.; Nowak, R. B.; Fowler, V. M.; Rangamani, P. Non-uniform distribution of myosin-mediated forces governs red blood cell membrane curvature through tension modulation. *PLOS Computational Biology* **2020**, *16*, No. e1007890.
(50) Alimohamadi, H.; Ovryn, B.; Rangamani, P. Modeling membrane nanotube morphology: the role of heterogeneity in composition and material properties. *Sci. Rep* **2020**, *10*, 2527.
(51) Molina, R. R.; Liese, S.; Alimohamadi, H.; Rangamani, P.; Carlson, A. Diffuso-kinetic membrane budding dynamics. *Soft Matter* **2020**, *16*, 10889−10899.
(52) Konar, S.; Arif, H.; Allolio, C. Mitochondrial membrane model: Lipids, elastic properties, and the changing curvature of cardiolipin. *Biophys. J.* **2023**, *122*, 4274−4287.
(53) Takei, K.; McPherson, P. S.; Schmid, S. L.; Camilli, P. D. Tubular membrane invaginations coated by dynamin rings are induced by GTP-γS in nerve terminals. *Nature* **1995**, *374*, 186−190.
(54) Liu, Y.-W.; Mattila, J.-P.; Schmid, S. L. Dynamin-Catalyzed Membrane Fission Requires Coordinated GTP Hydrolysis. *PLoS One* **2013**, *8*, No. e55691.
(55) Giacomello, M.; Pyakurel, A.; Glytsou, C.; Scorrano, L. The cell biology of mitochondrial membrane dynamics. *Nat. Rev. Mol. Cell Biol.* **2020**, *21*, 204−224.
(56) Derényi, I.; Jülicher, F.; Prost, J. Formation and interaction of membrane tubes. *Phys. Rev. Lett.* **2002**, *88*, 238101.
(57) Kozlovsky, Y.; Kozlov, M. M. Membrane fission: model for intermediate structures. *Biophys. J.* **2003**, *85*, 85−96.
(58) Roux, A.; Uyhazi, K.; Frost, A.; De Camilli, P. GTP-dependent twisting of dynamin implicates constriction and tension in membrane fission. *Nature* **2006**, *441*, 528−531.
(59) Ingerman, E.; et al. Dnm1 forms spirals that are structurally tailored to fit mitochondria. *J. Cell Biol.* **2005**, *170*, 1021−1027.
(60) Lackner, L. L.; Horner, J. S.; Nunnari, J. Mechanistic analysis of a dynamin effector. *Science* **2009**, *325*, 874−877.
(61) McDargh, Z. A.; Deserno, M. Dynamin's helical geometry does not destabilize membranes during fission. *Traffic* **2018**, *19*, 328−335.
(62) Stowell, M. H. B.; Marks, B.; Wigge, P.; McMahon, H. T. Nucleotide-dependent conformational changes in dynamin: evidence for a mechanochemical molecular spring. *Nat. Cell Biol.* **1999**, *1*, 27−32.
(63) Cagalinec, M.; et al. Principles of the mitochondrial fusion and fission cycle in neurons. *Journal of Cell Science* **2013**, *126*, 2187−2197.
(64) Berman, S. B.; et al. Bcl-xL increases mitochondrial fission, fusion, and biomass in neurons. *J. Cell Biol.* **2009**, *184*, 707−719.
(65) Dimova, R. Recent developments in the field of bending rigidity measurements on membranes. *Adv. Colloid Interface Sci.* **2014**, *208*, 225−234.
(66) Jin, A. J.; Prasad, K.; Smith, P. D.; Lafer, E. M.; Nossal, R. Measuring the Elasticity of Clathrin-Coated Vesicles via Atomic Force Microscopy. *Biophys. J.* **2006**, *90*, 3333.
(67) Baumgart, T.; Das, S.; Webb, W. W.; Jenkins, J. T. Membrane Elasticity in Giant Vesicles with Fluid Phase Coexistence. *Biophys. J.* **2005**, *89*, 1067−1080.
(68) Jülicher, F.; Lipowsky, R. Shape transformations of vesicles with intramembrane domains. *Phys. Rev. E* **1996**, *53*, 2670−2683.
(69) Hu, M.; Briguglio, J. J.; Deserno, M. Determining the Gaussian Curvature Modulus of Lipid Membranes in Simulations. *Biophys. J.* **2012**, *102*, 1403−1410.
(70) Dar, S.; Kamerkar, S. C.; Pucadyil, T. J. A high-throughput platform for real-time analysis of membrane fission reactions reveals dynamin function. *Nat. Cell Biol.* **2015**, *17*, 1588−1596.
(71) Bashkirov, P. V.; et al. GTPase Cycle of Dynamin Is Coupled to Membrane Squeeze and Release, Leading to Spontaneous Fission. *Cell* **2008**, *135*, 1276−1286.
(72) Morlot, S.; et al. Membrane Shape at the Edge of the Dynamin Helix Sets Location and Duration of the Fission Reaction. *Cell* **2012**, *151*, 619−629.
(73) Pucadyil, T. J.; Schmid, S. L. Real-Time Visualization of Dynamin-Catalyzed Membrane Fission and Vesicle Release. *Cell* **2008**, *135*, 1263−1275.
(74) Frohman, M. A. Role of mitochondrial lipids in guiding fission and fusion. *J. Mol. Med. (Berl)* **2015**, *93*, 263−269.
(75) Agrawal, A.; Ramachandran, R. Exploring the links between lipid geometry and mitochondrial fission: Emerging concepts. *Mitochondrion* **2019**, *49*, 305−313.
(76) Mahajan, M.; et al. NMR identification of a conserved Drp1 cardiolipin-binding motif essential for stress-induced mitochondrial fission. *Proc. Natl. Acad. Sci. U. S. A.* **2021**, *118*, No. e2023079118.
(77) Ugarte-Uribe, B.; Prévost, C.; Das, K. K.; Bassereau, P.; García-Sáez, A. J. Drp1 polymerization stabilizes curved tubular membranes similar to those of constricted mitochondria. *J. Cell Sci.* **2019**, *132*, jcs208603.
(78) Sorice, M.; et al. Cardiolipin-enriched raft-like microdomains are essential activating platforms for apoptotic signals on mitochondria. *FEBS Lett.* **2009**, *583*, 2447−2450.
(79) Ryan, T.; et al. Cardiolipin exposure on the outer mitochondrial membrane modulates α-synuclein. *Nat. Commun.* **2018**, *9*, 817.
(80) Montessuit, S.; et al. Membrane remodeling induced by the dynamin-related protein Drp1 stimulates Bax oligomerization. *Cell* **2010**, *142*, 889−901.
(81) Francy, C. A.; Alvarez, F. J. D.; Zhou, L.; Ramachandran, R.; Mears, J. A. The Mechanoenzymatic Core of Dynamin-related Protein 1 Comprises the Minimal Machinery Required for Membrane Constriction *. *J. Biol. Chem.* **2015**, *290*, 11692−11703.
(82) Bohuszewicz, O.; Low, H. H. Structure of a mitochondrial fission dynamin in the closed conformation. *Nat. Struct Mol. Biol.* **2018**, *25*, 722−731.
(83) Lee, C. T.; Venkatraman, K.; Budin, I.; Rangamani, P. Coupling between membrane undulations and lipid curvature leads to transient local enrichment of cardiolipin in mitochondrial membranes. *bioRxiv* **2025**, DOI: 10.1101/2025.01.17.633669.
(84) Deserno, M. Fluid lipid membranes: From differential geometry to curvature stresses. *Chem. Phys. Lipids* **2015**, *185*, 11−45.
(85) Yang, L.; et al. Mechanism of a prototypical synthetic membrane-active antimicrobial: Efficient hole-punching via interaction with negative intrinsic curvature lipids. *Proc. Natl. Acad. Sci. U. S. A.* **2008**, *105*, 20595−20600.
(86) Shnyrova, A. V.; et al. Geometric Catalysis of Membrane Fission Driven by Flexible Dynamin Rings. *Science* **2013**, *339*, 1433−1436.
(87) Merrifield, C. J.; Perrais, D.; Zenisek, D. Coupling between Clathrin-Coated-Pit Invagination, Cortactin Recruitment, and Membrane Scission Observed in Live Cells. *Cell* **2005**, *121*, 593−606.
(88) Cocucci, E.; Gaudin, R.; Kirchhausen, T. Dynamin recruitment and membrane scission at the neck of a clathrin-coated pit. *MBoC* **2014**, *25*, 3595−3609.
(89) Unsay, J. D.; Cosentino, K.; Subburaj, Y.; García-Sáez, A. J. Cardiolipin Effects on Membrane Structure and Dynamics. *Langmuir* **2013**, *29*, 15878−15887.
(90) Luo, E. W.-C.; et al. Drp1 Proteins Released from Hydrolysis-driven Scaffold Disassembly Trigger Nucleotide-dependent Membrane Remodeling to Promote Scission. *J. Am. Chem. Soc.* **2025**, DOI: 10.1021/jacs.4c15836.

https://doi.org/10.1021/jacs.5c06352
J. Am. Chem. Soc. XXXX, XXX, XXX−XXX

(91) Song, Y.; et al. Light-inducible deformation of mitochondria in live cells. *Cell Chemical Biology* **2022**, *29*, 109−119.
(92) Liu, X.; et al. Force-induced tail-autotomy mitochondrial fission and biogenesis of matrix-excluded mitochondrial-derived vesicles for quality control. *Proc. Natl. Acad. Sci. U. S. A.* **2024**, *121*, No. e2217019121.
(93) Kozlov, M. M. Fission of Biological Membranes: Interplay Between Dynamin and Lipids. *Traffic* **2001**, *2*, 51−65.
(94) Kozlov, M. M. Dynamin: Possible Mechanism of "Pinchase" Action. *Biophys. J.* **1999**, *77*, 604−616.
(95) Camley, B. A.; Brown, F. L. H. Beyond the creeping viscous flow limit for lipid bilayer membranes: Theory of single-particle microrheology, domain flicker spectroscopy, and long-time tails. *Phys. Rev. E* **2011**, *84*, 021904.
(96) Rahimi, M.; Arroyo, M. Shape dynamics, lipid hydrodynamics, and the complex viscoelasticity of bilayer membranes [corrected]. *Phys. Rev. E Stat Nonlin Soft Matter Phys.* **2012**, *86*, 011932.
(97) Rochon, K.; et al. Structural basis for regulated assembly of the mitochondrial fission GTPase Drp1. *Nat. Commun.* **2024**, *15*, 1328.
(98) Roux, A.; et al. Membrane curvature controls dynamin polymerization. *Proc. Natl. Acad. Sci. U. S. A.* **2010**, *107*, 4141−4146.
(99) Grassart, A.; et al. Actin and dynamin2 dynamics and interplay during clathrin-mediated endocytosis. *J. Cell Biol.* **2014**, *205*, 721−735.
(100) Anggono, V.; Robinson, P. J. Dynamin. *Encyclopedia of Neuroscience*; Elsevier, 2009; pp 725−735, DOI: 10.1016/B978-008045046-9.01363-2.
(101) Morlot, S.; Roux, A. Mechanics of dynamin-mediated membrane fission. *Annu. Rev. Biophys* **2013**, *42*, 629−649.

https://doi.org/10.1021/jacs.5c06352
J. Am. Chem. Soc. XXXX, XXX, XXX−XXX